Accepted Manuscript

Title: Adsorption mechanism of hexavalent chromium onto layered double hydroxides-based adsorbents: A systematic in-depth review

Authors: Hai Nguyen Tran, Dong Thanh Nguyen, Giang Truong Le, Fatma Tomul, Eder C. Lima, Seung Han Woo, Ajit K. Sarmah, Hung Quang Nguyen, Phuong Tri Nguyen, Duc Dinh Nguyen, Tien Vinh Nguyen, Saravanamuth Vigneswaran, Dai-Viet N. Vo, Huan-Ping Chao

PII: S0304-3894(19)30273-0
DOI: https://doi.org/10.1016/j.jhazmat.2019.03.018
Reference: HAZMAT 20399

To appear in: *Journal of Hazardous Materials*

Received date: 3 October 2018
Revised date: 5 February 2019
Accepted date: 4 March 2019

Please cite this article as: Tran HN, Nguyen DT, Le GT, Tomul F, Lima EC, Woo SH, Sarmah AK, Nguyen HQ, Nguyen PT, Nguyen DD, Nguyen TV, Vigneswaran S, Vo D-VietN, Chao H-Ping, Adsorption mechanism of hexavalent chromium onto layered double hydroxides-based adsorbents: A systematic in-depth review, *Journal of Hazardous Materials* (2019), https://doi.org/10.1016/j.jhazmat.2019.03.018

Adsorption mechanism of hexavalent chromium onto layered double hydroxides-based adsorbents: A systematic in-depth review

Hai Nguyen Tran[1]*, Dong Thanh Nguyen[2], Giang Truong Le[3], Fatma Tomul[4], Eder C. Lima[5], Seung Han Woo[6], Ajit K. Sarmah[7], Hung Quang Nguyen[1], Phuong Tri Nguyen[8], Duc Dinh Nguyen[9], Tien Vinh Nguyen[10], Saravanamuth Vigneswaran[10], Dai-Viet N. Vo[11], Huan-Ping Chao[12]*

[1]Institute of Fundamental and Applied Sciences, Duy Tan University, Ho Chi Minh City 700000, Vietnam

[2]Institute of Environmental Technology, Vietnam Academy of Science and Technology, Ha Noi, Vietnam

[3]Institute of Chemistry, Vietnam Academy of Science and Technology, Ha Noi, Vietnam

[4]Mehmet Akif Ersoy University, Faculty of Arts and Science, Chemistry Department, 15100 Burdur, Turkey

[5]Institute of Chemistry, Federal University of Rio Grande doSul (UFRGS), Porto Alegre, RS, Brazil

[6]Department of Chemical and Biological Engineering, Hanbat National University, 125 Dongseodaero, Yuseong-Gu, Daejeon 305-719, Republic of Korea

[7]Department of Civil & Environmental Engineering, Faculty of Engineering, The University of Auckland, Private Bag 92019, Auckland 1142, New Zealand

[8]Department of Chemistry, University of Montreal, Montreal, QC, Canada

[9]Department of Environmental Energy Engineering, Kyonggi University, Republic of Korea

[10]Faculty of Engineering and IT, University of Technology, Sydney (UTS), Sydney, Australia

[11]Faculty of Chemical & Natural Resources Engineering, Universiti Malaysia Pahang, Lebuhraya Tun Razak, Gambang 26300, Pahang, Malaysia

[12]Department of Environmental Engineering, Chung Yuan Christian University, Chung-Li 32023, Taiwan

---

Corresponding authors

Hai Nguyen Tran (trannguyenhai@duytan.edu.vn; trannguyenhai2512@gmail.com) at Duy Tan University , Vietnam

Huan-Ping Chao (hpchao@cycu.edu.tw) at Chung Yuan Christian University, Taiwan

Highlights

1. Properties and mechanisms of Cr(VI) adsorption onto LDH-based materials reviewed.
2. Such materials: high anion exchange capacity and positively charged external surface.
3. Identified mechanism: anion exchange, adsorption-coupled reduction, electrostatic attraction.
4. Adsorption-coupled reduction: identified by some advanced techniques from 2016.
5. Thermodynamic parameters: $\Delta G° < 0$, $\Delta H° > 0$, and $\Delta S° > 0$ in the most observation cases.

Table of Contents

Abstract

An attempt has been made in this review to provide some insights into the possible adsorption mechanisms of hexavalent chromium onto layered double hydroxides-based adsorbents by critically examining the past and present literature. Layered double hydroxides (LDH) nanomaterials are typical dual-electronic adsorbents because they exhibit positively charged external surfaces and abundant interlayer anions. A high positive zeta potential value indicates that LDH has a high affinity to Cr(VI) anions in solution through electrostatic attraction. The host interlayer anions (i.e., Cl^{-}, NO_3^{-}, SO_4^{2-}, and CO_3^{2-}) provide a high anion exchange capacity (53–520 meq/100g) which is expected to have an excellent exchangeable capacity to Cr(VI) oxyanions in water. Regarding the adsorption-coupled reduction mechanism, when Cr(VI) anions make contact with the electron-donor groups in the LDH, they are partly reduced to Cr(III) cations. The reduced Cr(III) cations are then adsorbed by LDH via numerous interactions, such as isomorphic substitution and complexation. Nonetheless, the adsorption-coupled reduction mechanism is greatly dependent on: (1) the nature of divalent and trivalent salts utilized in LDH preparation, and (2) the types of interlayer anions (i.e., guest intercalated organic anions). The low Brunauer–Emmett–Teller specific surface area of LDH (1.80–179 m^2/g) suggests that pore filling played an insignificant role in Cr(VI) adsorption. The Langmuir maximum adsorption capacity of LDH (Q^o_{max}) toward Cr(VI) was significantly affected by the used inorganic salt natures and synthetic methods of LDH. The Q^o_{max} values range from 16.3 mg/g to 726 mg/g. Almost all adsorption processes of Cr(VI) by LDH-based adsorbent occur spontaneously ($\Delta G° <0$) and endothermically ($\Delta H° >0$) and increase the randomness ($\Delta S° >0$) in the system. Thus LDH has much potential as a material that can effectively remove anion pollutants, especially Cr(VI) anions in industrial wastewater.

Keywords: Hexavalent chromium; layered double hydroxides; adsorption-coupled reduction; anion exchange; isomorphic substitution; critical review.

1. Introduction

Increase in the concentration of contaminants in surface water and groundwater due to various anthropogenic activities has become a serious issue worldwide. Most contaminants can generate an enormous health and public concern apart from adversely affecting aquatic organisms. Thus, they have to be removed from the aqueous environment. There are many methods by which they can be removed, such as adsorption, membrane process, and chemical precipitation. Among the existing method, adsorption has been acknowledged as widely acknowledged the most economically favourable technique. This is because adsorption method possesses several advantageous, such as high removal efficiency, simplicity in design, low operation cost, minimal generation of secondary by products (i.e., sludge formation) or transformation products, and feasibility for separating a wide range of pollutants from water media [1, 2]. Nanomaterials have been indentified as promising adsorbents in water and wastewater treatment has been highlighted recently [3, 4]. Similarly, layered

double hydroxides (LDH) with their average particle diameters (73–367 nm) are classified as colloidal nanoparticles [5]. However, the specific surface area of LDH (1.80–179 m^2/g) is often significantly lower than that of activated carbon (>1000 m^2/g), so pore filling is less significant than other processes (i.e., anion exchange and electrostatic attraction) in adsorption. Moreover, such biocompatible materials can serve as excellent dual-electronic adsorbents for adsorbing various potentially cationic and oxyanionic metal ions [6, 7] as well as organic anionic and cationic dyes [8, 9]. Furthermore, to easily separate the LDH nanoparticles from water solution, magnetic LDH nanosheets have been successfully synthesized [10, 11]. Therefore, LDH-based materials can be considered potential and promising adsorbents for removing various kinds of pollutant from the water environment.

In essence, layered double hydroxides are commonly known as hydrotalcite-like minerals or synthetic anionic clays. LDH compounds are classified as typically ionic layered materials because their structural characterization comprises positively charged brucite-like layers and non-framework charge compensating anions in their galleries (**Figure 1**). In other words, the brucite (magnesium hydroxide)-like layers include some divalent metal cations substituted by trivalent metal cations to form positively charged sheets [12]. Intercalating anions balance the positive charge in the interlayer regions of LDH. Some common interlayer anions (exchangeable or host anions), for example OH^-, Cl^-, ClO_4^-, SO_4^{2-}, CO_3^{2-}, and NO_3^-, have been previously documented in other studies (**Table S1**). The general form of LDH can be expressed in terms of the formula $[M^{2+}_{1-x}M^{3+}_x(OH)_2]^{x+}(A^{n-})_{x/n}\bullet mH_2O$; where: M^{2+} indicates divalent metal cations, M^{3+} is trivalent metal cations, A^{n-} represents the interlayer charge-balancing anions of valence *n*, and *x* is the $M^{3+}/(M^{2+} + M^{3+})$ molar ratio (ranges typically from 0.20 to 0.33) [13]. It is worth noting here that LDH nanomaterials exhibit versatile properties, in particular the "*memory effect*" (structure amenability) (**Figure 1**). It is this characteristic that makes them a promising adsorbent with high reversibility.

Figure 1

The ubiquitous presence of toxic oxyanions (e.g., arsenate and dichromate) in contaminated water sources is of particular concern in the treatment of drinking water. Hexavalent chromium Cr(VI)—a strong oxidizing agent—is a highly toxic chemical that can potentially cause dangerous health outcomes because of its carcinogenic and mutagenic nature and therefore, Cr(VI) removal from water requires urgent attention. As reported in the litearture, Cr(VI) anion in solution entirely/partly reduces to Cr(III) cation when it makes contact with an adsorbent's surface, for instance: natural biomaterial [14], amino-functionalized mesoporous ordered silica adsorbents [15], activated carbon [16], biochar [17], and nanoscale zero-valent iron modified with tetraethyl-ortho-silicate and hexadecyl-trimethoxy-silane [18]. Such an adsorbent can adsorb the reduced Cr(III) through various interactions (i.e., complexation). For this reason, the process they go through is known as "*adsorption-coupled reduction*" [14].

Recently, many scholars have applied some advanced techniques to explore the oxidation state of chromium bound to LDH. They concluded that the adsorption-coupled reduction mechanism is an integral aspect of Cr(VI) adsorption on LDH [10, 19-29]. More detail information on this mechanism is discussed in Section 5.2. However, such a mechanism is strongly dependent on the nature, property, and preparation method of LDH. Furthermore, the LDH adsorbents are uniquely characterized in such a way that they incorporate positively charged sites on their external surface (high positively ζ potential value) and abundantly exchangeable anions within their interlayers (high anion exchange capacity). Consequently, the role of anion exchange and electrostatic attraction of Cr(VI) oxyanions must be thoroughly understood and explicitly considered in the relevant research works. The overarching aim of this review is to explore the potential adsorption mechanism between toxic Cr(VI) oxyanions and LDH-based adsorbent with a particular focus on the role of anion exchange and electrostatic attraction of Cr(VI) oxyanions. A critical analysis of the available literature studies is presented with an emphasis on adsorption-coupled reduction process and a future perspective.

2. Some unique characteristics of layered double hydroxides

2.1. Morphological property and crystal structure

The characteristics of an adsorbent play an important role in determining its adsorption capacity and mechanism responsible in the removal of the pollutant from the media. In general, LDH is a hydrotalcite-like material with a hexagonal platelet-like morphology (**Figure 2a)**; its structural property indicates a typically well-crystallized nature. Obviously, the XRD spectrum of LDH (**Figure 2b**) shows two characteristic peaks at $2\theta = 11.6°$ and 23.2°, which correspond to the basal spacing and interlayer spacing of LDH, respectively [19]. The basal spacing (d_{003}) and an interlayer spacing (d_{006}) are primarily calculated based on Bragg's law. Notably, the existence of host carbonate anions in the interlayer region of LDH is commonly identified at a 2θ peak of nearly 30°. **Table S1** shows that the basal spacing of LDH (without any guest organic anions) strongly depends on the method of LDH preparation, used M(II) and M(III) salts, and M(II)/M(III) molar ratios.

Figure 2

2.2. Typical functional group

The presence of major functional groups on the hydrotalcite-like material is illustrated in **Figure 2c**. The LDH material exhibits a poor functionality with some identified peaks. Firstly, an extremely broad peak at approximately 3500 cm^{-1} is ascribed to the overlap of various types of O–H bonding vibrations, such as the hydroxyl groups in brucite-like layers, interlayer water molecules, and even physically adsorbed water [30]. Some recent analyses indicated that the protonated $–OH_2^+$ groups in the brucite-like sheets of LDH could complex with toxic metal cations (inner-sphere complexation) [19, 20]. Secondly, a well-identified peak at approximately 1650 cm^{-1} likely corresponds to the C=O and/or N=O functional groups formed from the internal anions (CO_3^{2-} and/or NO_3^-). Also, the C–O and/or N–O stretching vibrations of interlayer CO_3^{2-} or NO_3^- anions are observed at around 1380 cm^{-1}. Those exchangeable anions in the interlayer galleries can facilitate the

removal of toxic oxyanions from the solution through the anion-exchange mechanism. Lastly, a pronounced peak at about 680 cm^{-1} is designated for the lattice modes of O–M–O vibration [31, 32].

2.3. Zeta potential

As mentioned previously in **Section 1**, the LDH material contains brucite (magnesium hydroxide)-like layers with positively charged sheets which result from the abundant protonated hydroxyl groups (—OH_2^+) on its external surface. This means that LDH has a positive zeta potential within a wide solution pH range (**Figure 2d**). Similar to other colloids/adsorbents, LDH is characterized by the protonation and deprotonation of external surface functional groups (amphoteric feature). However, the zeta potential of LDH often indicates a high positive value, so the pH value of the isoelectric point of such material (pH_{IEP}) is often higher than 9.5. This includes, for example, Mg/Al-LDH (prepared by the alkoxide sol-gel method), Mg/Al-LDH (hydrothermal precipitation), and Mg/Al-LDH (alkoxide-free sol-gel synthesis) [33]. A high IEP value of Mg/Al-LDH probably result from the dissociation of mainly $Mg(OH)_2$ and some $Al(OH)_2^+$ sites [34]. A similar finding (**Table S2**) was reported elsewhere [5, 19, 28, 34, 35]. More interestingly, Tran et al. [31] found that the pH_{IEP} of LDH (higher than 12) is an insignificant change after intercalating with certain organic acid anions, such as citrate and malate anions. Because LDH possesses a high density and positively charged surface, it is expected to have a high affinity to anionic pollutants in solution.

2.4. Anion exchange capacity

Because LDH materials possess numerous exchangeable anions in their galleries as aforementioned, they generally exhibit an excellent anion exchange capacity (AEC). Consequently, they can serve as inorganic anion exchangers with a high affinity to various anionic pollutants in solution. For instance, Chubar et al. [33] reported that the LDH synthesis method strongly influences the ion exchange capacity on LDH. The AEC values of Mg/Al samples decrease in the following order: 450 meq/100g for the alkoxide-free sol-gel method > 400 meq/100g for the hydrothermal precipitation method > 300 meq/100g for the alkoxide sol-gel method [33]. Similarly, a high ACE of

Mg/Al hydrous oxides (450–520 meq/100g) was confirmed by Chubar [36]. In another study, Halajnia et al. [37] found that the anion exchange capacities of LDH were also strongly influenced by the M^{2+}/M^{3+} molar ratio, such as 0.89 mmol/g (3/1 Mg/Fe) > 0.88 mmol/g (4/1 Mg/Fe) and 1.93 mmol/g (3/1 Mg/Al) > 1.61 mmol/g (4/1 Mg/Al). Notably, Ramírez-Llamas et al. [38] pointed out that the AEC of Mg/Al-LDH (52.5 meq/100g) increased when the calcination temperature rose from 350 °C (75.0 meq/100g) to 450 °C (93 meq/100g) and then to 550 °C (127.5 meq/100g). Moreover, the AEC of Ni/Mg/Al-LDH material after the 500 °C calcination and H_2O expulsion was 210 meq/100g (or 33 meq/mol) as reported by Châtelet et al. [34].

2.5. Textural property

A typical nitrogen adsorption/desorption isotherm of LDH is presented in **Figure 2e**. According to the IUPAC classification, the isotherm is classed as an IV-type category with an obvious H3-type hysteresis loop at high relative pressure ($p/p_0 > 0.8$). The results indicated that the LDH possesses mesopores with slit-shaped pores that were formed by stacking the nanosheet building blocks [7, 9]. Similar findings have been reported in several other studies [8, 10, 24, 25, 33, 34, 39-42]. Generally, the LDH adsorbent can be classified as a non-porous material because of its poor porosity, implying that LDH often exhibits a low Brunauer–Emmett–Teller (BET) specific surface area (S_{BET}) and total pore volume (V_{Total}). According to the literature, the S_{BET} values of LDH that were prepared by different methods and salts ranged from 1.8 m^2/g to 179 m^2/g (**Table S3**). As a result, the role of pore filling in the adsorption of most contaminants onto LDH seems to be negligible [6, 7, 31].

Some important factors affecting the textural property of LDH include: (1) the M^{2+}/M^{3+} molar ratio of inorganic salts used in the synthesis of LDH, (2) calcination process, and (3) preparation method. For the first factor, the M^{2+}/M^{3+} molar ratio, its effect on the textural properties of LDH has been reported in the literature. Ling et al. [43] reported that the S_{BET} and V_{total} values of (NO_3)-Co/Fe-LDH decreased with an increase of Co/Fe molar ratio from 2:1 (168 m^2/g and 0.07 cm^3/g) to 3:1 (159

m^2/g and 0.0048 cm^3/g), and then to 4:1 (109 m^2/g and 0.0047 cm^3/g), respectively. This outcome is similar to the findings of some authors [25, 26, 37]; however, in contrast to the findings of Peng et al. [44].

For the second factor, calcination process, the S_{BET} of LDH is generally enhanced during calcination under atmospheric air (also known as the dehydration, dehydroxylation and phase transition of LDH) [45]. Porosity occurs following calcination due to the decomposition of LDH into metal oxides with a periclase-like structure. For example, Ramírez-Llamas et al. [38] have found that the S_{BET} (m^2/g) and V_{Total} (cm^3/g) values of (SO_4)-Mg/Al-LDH (95 m^2/g and 0.28 cm^3/g) greatly increased after being calcined at 350 °C (142 m^2/g and 0.42 cm^3/g), 450 °C (180 m^2/g and 0.64 cm^3/g), and 550 °C (216 m^2/g and 1.02 cm^3/g). Analogous results (**Table S4**) have been observed by some other researchers [8, 34, 40, 42, 46].

Furthermore, the reconstruction of the original Mg/Al-LDH structure is often known as the "*memory effect*" term. The gas-phase and liquid-phase rehydrations of calcined LDH also exert positive or negative effects on the textural properties of LDH (**Table S4**). Lastly, the effect of the last factor (the preparation method) on the textual properties of LDH is summarized in **Table S3**.

3. Distribution of Cr(VI) species in solution

Aqueous hexavalent chromium often exists in the form of different species (H_2CrO_4, $HCrO_4^-$, CrO_4^{2-}, $Cr_2O_7^{2-}$, and $HCr_2O_7^-$) as a function of solution pH levels and total chromium concentrations (**Figure 3**). For example, a potent oxidizing agent (chromic acid; H_2CrO_4) is primarily found in solution at a pH level below 1.0, while hydrogen chromate ($HCrO_4^-$) anion is the dominant anionic chromium species in a solution within the 1.0 to 6.0 pH range. In addition, Cr(VI) exists mainly as the anionic species of chromate (CrO_4^{2-}) when solution pH >6.0 [14, 47]. Remarkably, as initially reported by Sengupta and Clifford [48] in **Figure 3b**, dichromate ($Cr_2O_7^{2-}$) anion, which is a dimer of $HCrO_4^-$, is commonly formed when the chromium concentration exceeds approximately 1000 mg/L. This accords with what previous studies have reported elsewhere [49, 50].

Figure 3

4. Possible adsorption mechanism

4.1. Anion exchange

Anion exchange between host anions in the interlayer region of LDH and certain pollutant anions in solution has been acknowledged as the primary adsorption mechanism. As noted in **Section 1** and **Table S1**, the existence of anionic types in the interlayer position of LDH is strongly dependent on the kinds of bivalent and trivalent salts used in LDH synthesis. A typical example was taken by Lazaridis et al. [51] for the preparation of (CO_3)-Mg/Al-LDH from $Mg(NO_3)_2 \bullet 6H_2O$ and $Al(NO_3)_3 \bullet 9H_2O$ through the traditional co-precipitation method. They proposed the anion-exchange mechanism for Cr(VI) adsorption by (CO_3)-Mg/Al-LDH can be described by the following equations:

$$Mg_6Al_{l2}(OH)_{16}CO_3 \bullet 4H_2O + 2HCrO_4^- \rightleftharpoons Mg_6Al_2(OH)_{16}(HCrO_4)_2 \bullet xH_2O + CO_3^{2-} \quad (1)$$

$$Mg_6Al_{l2}(OH)_{16}CO_3 \bullet 4H_2O + CrO_4^{2-} \rightleftharpoons Mg_6Al_2(OH)_{16}CrO_4 \bullet yH_2O + CO_3^{2-} \quad (2)$$

According to the XRD data, Cocheci et al. [30] found that the interlayer carbonate anions in calcinated (CO_3)-Zn/Al–LDH were not replaced by Cr(VI) anions during the adsorption process, suggesting that the anion exchange might be not mainly responsible for Cr(VI) adsorption in aqueous solution. The Langmuir maximum adsorption capacity (Q^o_{max}) of LDH declined according to the calcination temperatures as follows: 0 °C > 250 °C > 300 °C > 500 °C. The highest adsorption capacity of (CO_3)-Zn/Al–LDH was caused by the significant contribution of anion-exchange mechanism, which was confirmed by the peak disappearing at nearly 30° in the XRD spectrum of laden-LDH. A similar adsorption tendency was reported by Khitous et al. [46], however elsewhere, the result was in stark contrast to those reported by several others researchers [8, 42, 52]. The varying adsorption trends might be due to these studies' unique LDH property or preferred primary adsorption mechanism. For example, Lei et al. [8] successfully synthesized the hierarchical hollow Ni/Mg/Al-layered double hydroxides (NMA-LDH) microspheres and (600 °C)-calcinated NMA-LDH (also

known as Ni/Mg/Al-layered double oxides; NMA-LDO). The Langmuir maximum adsorption capacity of NMA-LDO was approximately twice higher than that of the NMA-LDH. Unlike the conventional morphology of LDH (a hexagonal platelet-like morphology) [30], the NMA-LDH and NMA-LDO materials exhibited the morphology of hierarchical flower-like hollow microspheres. The dissimilar morphology can cause the different adsorption tendency between pristine and calcinated LDH samples.

Moreover, the (NO_3)-Co/Fe-LDH adsorbent, which was successfully prepared by co-precipitating the mixed metal solutions of $Co(NO_3)_2•6H_2O$ and $Fe(NO_3)_3•9H_2O$, exhibited an outstanding anion exchange capacity to Cr(VI) in solution [43]. The XRD data of (NO_3)-Co/Fe-LDH indicated that the peak corresponding to the presence of CO_3^{2-} anions in the interlayer region of LDH was not detected, implying that the existence of interlayer CO_3^{2-} anions was negligible. Also, the basal spacing of (NO_3)-Co/Fe-LDH increased from 0.804 to 0.900 nm after adsorption, which is later confirmed by other findings reported in **Table S1**. The results suggested that the interlayer NO_3^- anions (the 0.20-nm radius) were primarily exchanged by $Cr_2O_7^{2-}$ oxyanions (0.24 nm) in solution. A similar performance of anion exchange is reported by Deng et al. [11] using magnetic $CoFe_2O_4$-Mg/Al-LDH composite and Koilraj and Sasaki [21] using (NO_3)-Mg/Al-LDH, (NO_3)-Co/Al-LDH, and (NO_3)-Zn/Al-LDH.

Notably, Khitous et al. [46] compared the removal efficacy of Cr(VI) from aqueous solution by three Mg/Al-LDH samples (NO_3-LDH, SO_4-LDH, and Cl-LDH) containing different interlayer NO_3^-, SO_4^{2-}, and Cl^- anions, respectively. Their Langmuir maximum adsorption capacities decreased in the following order: 71.9 mg/g (NO_3-LDH) > 58.8 mg/g (Cl-LDH) > 55.6 mg/g (SO_4-LDH). An analogous tendency was observed by Hongo et al. [53] for Cr(VI) adsorption onto Mg/Al-LDH samples with different interlayer anions: $NO_3^- > Cl^- > SO_4^{2-}$. The result suggested that the interlayer NO_3^- anions exhibited a superior exchangeable capacity to Cr(VI) anions in the solution than the interlayer Cl^- and SO_4^{2-} anions did. In other words, the host divalent anions more strongly interacted in the interlayer region of LDH than the host monovalent anions. Moreover, the anion-

exchange mechanism between the guest Cr(VI) anions and the host Cl^- anions in the interlayer region of LDH has been highlighted by many scholars [25, 32, 54].

To sum up, the anion exchange mechanism is strongly dependent on the preparation of LDH and the salt used. For example, if the LDH sample is synthesized by the coprecipitation method of two metal salts (i.e., $MgSO_4$ and $Al_2(SO_4)_3$) using nitrogen gas to minimize the presence of CO_3^{2-} anions in the solution, the anion exchange mechanism between Cr(VI) in solution and the interlayer anions of LDH will be negligible. This is because (1) the presence of exchangeable CO_3^{2-} anions in the interlayer anions of LDH is limited, and (2) interlayer SO_4^{2-} anions are difficult to exchange with Cr(VI) anions in solution.

4.2. Adsorption-coupled reduction

When Cr(VI) oxyanions in solution come into contact with certain organic substances or reducing agents (especially in acidic environments), the Cr(VI) species are easily transformed/reduced to Cr(III) species according to a redox mechanism. This reason is that Cr(VI) has a high redox (oxidation/reduction) potential value (usually higher than +1.35 V) under standard conditions [55]. As reported in the literature, when Cr(VI) oxyanions make contact with the electron-donor groups of adsorbent (i.e., the hydroxyl group), Cr(VI) is spontaneously reduced to Cr(III). LDH can adsorb the reduced Cr(III) cations through isomorphic substitution and complexation. X-ray photoelectron spectroscopy (XPS), X-ray absorption spectroscopy (XAS), and extended X-ray absorption fine structure (EXAFS) are three useful advanced techniques to ascertain the oxidation state of the chromium bound on the adsorbent. These methods can be used to identify whether: firstly, Cr(VI) is totally or partially reduced to Cr(III) during Cr(VI) adsorption; and secondly, reduced Cr(III) is adsorbed onto adsorbent or not.

Figure 4a provides the results for XPS analysis of standard Cr(III) chemical ($CrCl_3 \cdot 6H_2O$ and Cr_2O_3) and standard Cr(VI) chemical ($K_2Cr_2O_7$) that were adapted from literature reports [16, 17, 23, 56, 57]. The standard chemicals were measured by XPS as blank samples without the presence of

adsorbent. Hexavalent chromium is always characterized by the peaks located at the higher binding energies than those of trivalent chromium. This is because hexavalent chromium is more electrophilic [56, 58]. Notably, the XPS analysis of the standard Cr(III) and Cr(VI) chemicals plays a key role in comparing the chromium states present on the adsorbent. The incorrect identification of Cr(III) and Cr(VI) binding energies in the Cr 2p XPS spectra of laden adsorbent will lead to incorrect conclusion. This problem has been recently identified and thoroughly discussed by Tran [58] and Tran et al. [59]

Figure 4

4.2.1. Layered double hydroxides without guest organic/inorganic anions or iron composition

Chen et al. [20] prepared the LDH modified by biomass-derived porous carbons (Ni/Al-LDH@PAB) to remove Cr(VI) anions from aqueous solution. The XPS narrow-spectrum of Cr 2p of Cr(VI)-laden Ni/Al-LDH@PAB confirmed that Cr(VI) and Cr(III) coexist on the surface and/or the interlayer region of Ni/Al-LDH@PAB. The authors demonstrated that some Cr(VI) anions were reduced to Cr(III) cations. During the reduction process, the large amount of hydroxyl groups on the surface of activated carbon and Ni/Al-LDH was responsible for donor electrons. The dominant presence of reduced Cr(III) on Ni/Al-LDH@PAB was due to two adsorption mechanisms, i.e. isomorphic substitution and complexation. Isomorphic substitution can be generated in the LDH structure because Cr^{3+} (0.052 nm) and Al^{3+} (0.054 nm) have a similar radius; consequently, the presence of Al^{3+} ions in the supernatant solution was detected around 0.84 mg/L after Cr(VI) adsorption. The complexation of the formed Cr(III) with oxygen-containing groups was another interaction. An analogous result was reported by Zhang et al. [60] for Cr(VI) adsorption onto (Cl)-Ca/Al-LDH.

Recently, Chao et al. [19] developed a novel method to remove toxic Cr(VI) from groundwater (containing soil) by CO_3-Mg/Al-LDH using characteristics of *in-situ* synthesis. The *in-situ* LDH can directly remove hexavalent chromium from solution through primary anion exchange with host interlayer anions (mainly CO_3^{2-}) and adsorption-coupled reduction mechanism. Three LDH

samples were synthesized at different concentrations of $Mg(NO_3)_2 \bullet 6H_2O$ and $Al(NO_3)_3 \bullet 9H_2O$ (the molar ratio of Mg/Al is 3:1). The XRD data of three LDH samples indicated that the peak corresponding to interlayer CO_3^{2-} anions was not detected, suggesting that anion exchange in adsorption mechanism is important. The XPS data (the O 1s and N 1s spectra) confirmed that anion exchange was unfavorable between interlayer NO_3^- anions and guest Cr(VI) anions in solution. Furthermore, they also indicated that some Cr(VI) oxyanions (approximately 20%) are reduced to Cr(III) cations at a high solution pH of 12 by the –OH groups in LDH or organic matter in silty clay. The coexistence of Cr(III) and Cr(VI) in LDH was confirmed by the Cr 2p spectrum (**Figure 4b**) at 587.9 eV and 579.1 eV for Cr(VI) and at 585.1 eV and 576.5 eV for Cr(III). The mechanism of isomorphic substitution between reduced Cr(III) and Al(III) was supported by a remarkable decline of the Mg/Al ratios (ranging from 1.40 to 1.82; determined by XPS).

4.2.2. Layered double hydroxides intercalated with organic/inorganic anions

Koilraj and Sasaki [21] investigated the adsorption behavior of Cr(VI) onto three different amino acid-intercalated LDH samples (i.e., Co/Al-LDH and Mg/Al-LDH) utilizing the XPS technique (**Figure 4c**). The existence of Cr(VI) and Cr(III) on the LDH samples was identified in the Cr 2p region at 578.3 eV and 587.4 eV for Mg/Al-LDH and at 578.8 eV and 588.0 eV for Co/Al-LDH. Meanwhile, that of Cr(III) was at 575.8 eV and 575.8 eV (Mg/Al-LDH) and at 576.5 eV and 585.5 eV (Co/Al-LDH), respectively. The Cr(III) present in Mg/Al-LDH and Co/Al-LDH was 44% and 19%, respectively, implying the partial detoxification of Cr(VI) by reduction to Cr(III) on the surface of the LDH samples. During the reduction process, the electron donating amine groups in amino acid can be oxidized to the –NH(OH) hydroxylamine derivation (**Equation 3**). The converted Cr(III) is unstable and precipitated in the CrOOH formation that was immobilized on the surface of LDH. More interestingly, after chromium-laden Mg/Al-LDH was desorbed by 0.01 M Na_2CO_3, two (Cr $2p_{3/2}$ and Cr $2p_{1/2}$) peaks corresponding to Cr(VI) disappeared in the Cr 2p spectrum. It is suggested here that anion exchange has played a determining role in adsorbing Cr(VI).

$$CrO_4^{2-} + 8H^+ + 3e^- (-NH_2) \rightleftharpoons Cr^{3+} + -NH(OH) + H_2O \quad (3)$$

Moreover, Zhang et al. [22] prepared the lactate acid-intercalated Mg/Al LDH nanocomposite (LDHNS) through the following three-stage process: (1) traditional co-precipitation method of $Mg(NO_3)_2 \bullet 6H_2O$ and $Al(NO_3)_3 \bullet 9H_2O$ to prepare NO_3-Mg/Al-LDH; (2) anion exchange between NO_3^- and lactate acid; and (3) exfoliation process. The XPS spectrum of LDHNS after adsorption of 100 mg/L of Cr(VI) for 10 min at pH 6.0 revealed some peaks at 576.3 eV [Cr(III)], 577.9 eV [Cr(VI)], and 587.2 eV [Cr(VI)], suggesting that Cr(III) was derived from Cr(VI) reduction. The intercalated lactate molecules (mainly –OH groups) within the galleries of LDHNS can serve as a potential reducer for partial reduction of Cr(VI) to Cr(III). The generated Cr(III) ions were adsorbed by the —COO^- groups of the lactate. Moreover, Zhang et al. [22] concluded "the hydrogen bonding between the Cr(VI)/Cr(III) species and the hydroxyl groups of the LDHNS." This means that the hydrogen bonding are responsible for the adsorption of Cr(VI) and/or Cr(III) onto LDHNS. However, this very controversial conclusion was withdrawn without any supporting experiment data.

Similarly, Deng et al. [10] fabricated the $NiFe_2O_4$/Zn-Al layered double hydroxides intercalated with ethylenediamine tetra-acetic acid (EDTA). After Cr(VI) adsorption, the XPS data indicated the coexistence of Cr(VI) and Cr(III) on the fabricated LDH (**Figure 4d**). The authors concluded that the C–H and C=O groups (the strongest reducing groups) were mainly responsible for the reduction of Cr(VI) to Cr(III) as depicted in **Equations 4–5**. The generated Cr(III) cations in solution possibly interacted with the negatively charged EDTA in the internal region of LDH to form a stable complex. After such adsorbing sites had become exhausted, the reduced Cr(III) cations were released into the solution because of the electronic repulsion between the reduced Cr(III) cations and the positively charged groups (—OH_2^+) on the surface of LDH.

$$-C-H + Cr(VI) + H_2O \rightleftharpoons -C-OH + Cr(III) + H^+ \quad (4)$$

$$-C=O + Cr(VI) + H_2O \rightleftharpoons -COOH + Cr(III) + H^+ \quad (5)$$

Furthermore, Ma et al. [23] synthesized the Mg/Al-LDH intercalated with inorganic MoS_4^{2-} anions (MoS_4-LDH) and applied the XPS technique to investigate the primary adsorption mechanism. The preparation of MoS_4-LDH comprised the following stages. Firstly, highly crystallized CO_3-Mg/Al-LDH was prepared through the traditional co-precipitation method. Secondly, the NO_3-LDH sample was then prepared by the decarbonization of CO_3-Mg/Al-LDH via a salt-acid mixed solution treatment. Thirdly and lastly, the Mg/Al-LDH intercalated with MoS_4^{2-} anions (MoS_4-LDH) was obtained through an anion exchange process between MoS_4^{2-} anions and interlayer NO_3^- anions in NO_3-LDH. The XPS result of MoS_4-LDH after Cr(VI) adsorption of 50 mg/L concentration indicated the Cr $2p_{2/3}$ and Cr $2p_{1/2}$ binding energies at 577.2 eV and 586.9 eV, corresponding to Cr(III). This means that during the Cr(VI) adsorption process, Cr(VI) was reduced to Cr(III) by a heterogeneous redox process. The reduced Cr(III)—a softer Lewis acid—might combine with the interlayer MoS_4^{2-} anions through the Cr−S coordination bonding. Furthermore, Ma et al. [23] discovered that the partial oxidation of S^{2-} to SO_4^{2-} anions simultaneously resulted in the reduction of Cr(VI) to Cr(III). This oxidation was confirmed by a well-indentified peak at 168.0 eV, involving the S 2p binding energy for SO_4^{2-}.

4.2.3. Layered double hydroxides modified with polymer

A polyaniline-modified Mg/Al-LDH, which was synthesized and applied to adsorb Cr(VI), was studied by Zhu et al. [24]. The Cr 2p XPS spectrum of Cr-loaded LDH indicated that the oxidation state of Cr(III) existed along with Cr(VI), implying that reduction occurred during Cr(VI) adsorption. The dominant reaction between acid chromate ($HCrO_4^-$) anions and polyaniline polymer is presented as **Equation 6.** The reduced Cr(III) species might be attached to the LDH surface by chelating with the amine groups of polyaniline (**Equations 7–9**). An identical result was reported by Deng and Ting [61] for Cr(VI) adsorption onto polyethyleneimine-modified fungal biomass and Olad and Nabavi [62] for polyaniline (PANI) application in the reduction of highly toxic Cr(VI) to less toxic Cr(III) ions in aqueous media.

$$2HCrO_4^- + 14H^+ + 3PANI^0 \rightleftharpoons 2Cr^{3+} + 3PANI^{2+} + 8H_2O \quad (6)$$

$$—NH_2 + Cr^{3+} \rightleftharpoons —NH_2Cr^{3+} \quad (7)$$

$$—NH_2 + Cr(OH)^{2+} \rightleftharpoons —NH_2Cr(OH)^{2+} \quad (8)$$

$$—NH_2 + Cr(OH)^{+} \rightleftharpoons —NH_2Cr(OH)^{+} \quad (9)$$

4.2.4. Layered double hydroxides containing an iron component

The Fe/Al layered double hydroxides were successfully synthesized by He et al. [25] through the hydrothermal synthesis method using $FeCl_2•4H_2O$ and $AlCl_3•6H_2O$. The XPS spectra of Fe/Al-LDH before and after adsorption indicated that Fe^{2+} ions in the LDH structure were simultaneously oxidized to Fe^{3+} ions. This action promoted the transformation of Cr(VI) into Cr(III). Furthermore, the concentration of Cr(III) cations in the solution during Cr(VI) adsorption was detected, suggesting that some reduced Cr(III) was released from the LDH sample during the adsorption process. Similarly, Kameda et al. [63] prepared the (Cl)-Mg/Al-LDH doped with Fe^{2+} (LDH-Fe), in which Fe^{2+} served as the strong reducing agent. They found that during the Cr(VI) adsorption process, the Fe^{2+} in the LDH-Fe host layer was oxidized into Fe^{3+}; this oxidation process can provide the electrons for simulating the reduction of Cr(VI) into Cr(III). A similar phenomenon was repeated by Alidokht et al. [26] for removing chromate from aqueous media by reduction with nanoscale (Cl)-Fe/Al-LDH.

$$Fe^{2+} \rightleftharpoons Fe^{3+} + e^- \quad (10)$$

$$Cr_2O_7^{2-} + 14H^+ + 6e^- \rightleftharpoons 2Cr^{3+} + 7H_2O \quad (11)$$

In another study, Wang et al. [27] successfully synthesized Mg/Al/Fe-LDH from $Mg(NO_3)_2$, $Al(NO_3)_3$, and $FeSO_4$. The XPS data indicated that the oxidation of Fe(II) to Fe(III) occurred during Cr(VI) adsorption. They found that the laminate Fe(II) in Mg/Al/Fe-LDH promoted the transformation of Cr(VI) into Cr(III). The reduced Cr(III) was removed through the formation of $Cr(OH)_3$. The hypothesis was

consistent with the Cr 2p spectrum in that Cr(VI) and Cr(III) coexist in Mg/Al/ Fe-LDH. The results suggested that the mechanism of Cr(VI) removal by Mg/Al/ Fe-LDH was regarded as a combination of adsorption–reduction processes.

Furthermore, Sheng et al. [28] synthesized the nanoscale zero-valent iron (NZVI) supported on Mg/Al-LDH (NZVI/LDH) and applied them (NZVI, LDH, and NZVI/LDH) to remove Cr(VI) in the liquid phase. The adsorption mechanism was proposed based on X-ray absorption fine structure (XAFS; **Figure 5a**) and extended X-ray absorption fine structure (EXAFS; **Figure 5b**) techniques. The XANES and EXAFS spectra of Cr-laden LDH are nearly identical to those of standard Cr(VI) chemical ($K_2Cr_2O_7$), suggesting that Cr(VI) does not reduce to Cr(III) during the Cr(VI) adsorption process onto Mg/Al-LDH. In contrast, the Cr-laden NZVI/LDH sample exhibited similar XANES and EXAFS patterns to the standard Cr(III) chemical, suggesting that Cr(VI) anions in solution were completely reduced to Cr(III) in the NZVI/LDH system. The reduction process occurred very rapidly within 15 min of contact. As part of their study, Sheng et al. [28] also found that Cr(VI) anions were only partly reduced to Cr(III) in the NZVI system. Notably, the reduction of Cr(VI) to Cr(III) by the nanoscale zero-valent iron (NZVI)-based adsorbent has been observed in the literature, such as activated carbon fiber supported-NZVI [64] and NZVI modified with tetraethyl orthosilicate and hexadecyl-trimethoxy-silane [18]. The NZVI reductant is known to be an excellent electron donor because of its great ability to lose electrons. According to [18, 64], the reduction of Cr(VI) to Cr(III) induced by NZVI can be summarized as follows:

$$3Fe^0 + 2HCrO_4^- + 14H^+ \rightleftharpoons 3Fe^{2+} + 2Cr^{3+} + 8H_2O \quad (11)$$

$$3Fe^{2+} + HCrO_4^- + 7H^+ \rightleftharpoons 3Fe^{3+} + Cr^{3+} + 4H_2O \quad (12)$$

$$Fe^0 \rightleftharpoons Fe^{2+} + 2e^- \quad (13)$$

$$Fe^0 + 2Fe^{3+} \rightleftharpoons 3Fe^{2+} \quad (14)$$

$$3Fe^0 + 2CrO_4^{2-} + 8H_2O \rightleftharpoons 3Fe^{2+} + 2Cr^{3+} + 16OH^- \quad (15)$$

$$3Fe^{2+} + CrO_4^{2-} + 4H_2O \rightleftharpoons 3Fe^{3+} + Cr^{3+} + 8OH^- \quad (16)$$

Figure 5

Notably, Laipan et al. [29] attempted to convert Orange II dye-laden (NO_3)-Cu/Fe-LDH into Cr(VI) reductant. According to the Cr 2p XPS data, these researchers concluded that approximately 71.4%–83.3% of Cr(III) presented in the Cr(VI)-laden LDH, suggesting that the adsorption-coupled reduction played a dominant role in this case. In addition, the Fe^0, Fe^{2+}, Cu^0, and Cu^+ species made a great contribution to reducing Cr(VI) to Cr(III) during the Cr(VI) adsorption process (based on the XPS analysis). The process of Cr(VI) reduction, which resulted from the reactions between Cr(VI) and such species, can be summarized as follows:

$$Cr_2O_7^{2-} + 14H^+ + 3(2)Fe^0 \rightleftharpoons 2Cr^{3+} + 7H_2O + 3Fe^{2+}(2Fe^{3+}) \quad (17)$$

$$Cr_2O_7^{2-} + 14H^+ + 6Fe^{2+} \rightleftharpoons 2Cr^{3+} + 7H_2O + 6Fe^{3+} \quad (18)$$

$$Cr_2O_7^{2-} + 14H^+ + 3(6)Cu^0 \rightleftharpoons 2Cr^{3+} + 7H_2O + 3Cu^{2+}(6Cu^+) \quad (19)$$

$$Cr_2O_7^{2-} + 14H^+ + 6Cu^+ \rightleftharpoons 2Cr^{3+} + 7H_2O + 6Cu^{2+} \quad (20)$$

However, using the XPS data after Cr(VI) adsorption, some authors detected that Cr(VI) did not reduce to Cr(III) during the adsorption process. For example, Yuan et al. [65] prepared a calcined graphene/Mg/Al-LDH nanocomposite. Their XPS spectrum for Cr 2p only presented one peak at 280 eV, meaning that the process of Cr(VI) removal by the prepared LDH nanocomposite did not involve the adsorption-coupled reduction. A similar conclusion was reached by Lei et al. [8] for the hierarchical calcined Ni/Mg/Al-LDH, Deng et al. [11] for the magnetic $CoFe_2O_4$/Mg/Al-LDH composite, and Wang et al. [66] for the polyvinylpyrrolidone- and polyacrylamide-intercalated LDH samples.

4.3. Electrostatic attraction

As discussed in **Section 1,** the LDH samples exhibited a positively charged surface that mainly resulted from the OH_2^+ groups present on its structure. Therefore, the electrostatic attraction between the OH_2^+ groups and Cr(VI) anions in solution was expected to occur naturally (**Figure 6c**). Such a mechanism has been confirmed by many investigators for the following: $NiFe_2O_4$-Zn/Al-LDH intercalated with EDTA [10], *in-situ* Mg/Al-LDH [19], (NO_3)-Mg/Al–LDH [46], (CO_3)-Mg/Al–LDH [28], magnetic $CoFe_2O_4$/MgAl-LDH [11], (NO_3)-Mg/Al–LDH and (500 °C)-calcinated Mg/Al–LDH [52], (Cl)-Zn/Al-LDH [35], and polyvinylpyrrolidone-intercalated LDH and polyacrylamide-intercalated LDH [66]. Although electrostatic attraction plays an integral role in adsorbing Cr(VI) anions in solution, its contribution might be not significant compared to anion exchange and adsorption coupled with reduction. The potential mechanisms of Cr(VI) adsorption onto LDH-based materials are summarized in **Figure 7.**

Figure 6

5. Discussion on the method for determining chromium

Following the Cr(VI) adsorption process, hexavalent and trivalent chromium can coexist in the solution and on the adsorbent if the reduction of Cr(VI) to Cr(III) occurs during the adsorption process. Many scholars [58, 59, 67-71] have discussed on the mistakes in analyzing chromium species in water environment (liquid phase) and on the laden adsorbent (solid phase) after the process of Cr(VI) adsorption. This mistake caused the incorrect explanation of mechanism adsorption. To prevent the proliferation of such mistakes in the future literature, this review recommends the accurate determination methods to verify their coexistence in both liquid and solid phases that are summarized in **Figure 7**.

Figure 7

Essentially, total (trivalent and hexavalent) chromium in solution is commonly determined using two techniques, specifically, inductively coupled plasma-atomic emission spectroscopy (ICP-AES), and atomic absorption spectroscopy (AAS). However, these methods cannot differentiate Cr(VI) from total chromium. The standard colorimetric method has been widely applied to measure the chromium concentration of its different species [Cr(VI) and total Cr concentrations] in solution. For example, to separate Cr(VI) and Cr(III) in a solution, sole Cr(VI) in solution is complexed with 1,5-diphenyl-carbazide, and the UV-visible spectroscopy technique is then used to detect the violet colored complex at the maximum absorption wavelength of 540 nm. For measuring total chromium, it is necessary to completely convert Cr(III) in solution into Cr(VI) at a high temperature (130–140 °C) by adding an oxidation treatment with $KMnO_4$. As a result of this oxidation treatment, the total concentration of hexavalent chromium consists of both the converted Cr(VI) oxyanions and the previously existing Cr(VI) oxyanions. Furthermore, the Cr(VI) oxyanions are complexed with 1,5-diphenyl-carbazide, and this complex is spectrophotometrically determined at 540 nm. Notably, the Cr(III) concentration is commonly calculated from the difference between the total Cr and Cr(VI) concentrations [15, 72-74].

According to the literature, the oxidation state and coordination environment of chromium bound to adsorbent is accurately confirmed by some advanced techniques, such as X-ray photoelectron spectroscopy (XPS) [10, 16, 17, 21, 56, 58, 75] and X-ray absorption fine structure (XAFS) [28, 76, 77]. If Cr(III) cations are not detected in solution and on laden adsorbent after Cr(VI) adsorption, Cr(VI) would not reduce to Cr(III). In contrast, it is also able to assume that the Cr(VI) reduces to Cr(III) during Cr(VI) adsorption. We analyze two possible cases where this can occur. Firstly, the reduced Cr(III) and Cr(VI) are detected in the solution. This means that the reduced Cr(III) cations are released to solution: (1) without adsorption onto adsorbent (invisible Cr(III) peak in XPS); or (2) with adsorption onto adsorbent (visible Cr(III) peak in XPS). In the second possibility, the adsorption however does not completely occur because of the limited adsorption capability of absorbent (insufficient reaction). Secondly, only Cr(VI) anions are detected in the solution. If the

XPS can determine the presence of Cr(III) on the laden adsorbent, this means that all reduced Cr(III) is adsorbed onto the adsorbent (sufficient reaction) [17, 58, 68, 77]. More information on such helpful techniques is previoulsy presented in **Section 4.2**.

6. Adsorption study

The study of equilibrium adsorption plays a significant role in estimating the maximum adsorption capacity of adsorbent under optional operation conditions [78, 79]. When the adsorption process reaches true equilibrium adsorption in the adsorption isotherm, the Langmuir model (**Equation 21**) is widely applied to calculate the maximum adsorption capacity of an adsorbent [70, 80]. Another equation (**Equation 22**) is commonly used to calculate the amount of Cr(VI) adsorbed onto adsorbent at equilibrium (q_e; mg/g).

$$q_e = \frac{Q^o{}_{\max} K_L C_e}{1 + K_L C_e} \tag{21}$$

$$q_e = \frac{C_o - C_e}{m} V \tag{22}$$

where $Q^o{}_{max}$ (mg/g) is the Langmuir maximum saturated adsorption capacity of LDH; K_L (L/mg) is the Langmuir constant related to the affinity between LDH and dichromate; C_o and C_e are the Cr(VI) concentration in the solutions at the beginning and equilibrium, respectively; m (g) is a used mass of LDH; and V (L) is the volume of the Cr(VI) solution.

Table 1 summarizes the Langmuir maximum adsorption capacity ($Q^o{}_{\max}$; mg/g) of different kinds of LDH adsorbent. The $Q^o{}_{\max}$ values of LDH-based materials range from 16.3 mg/g to 726 mg/g, which are comparable to some commercial anion exchangers, such as Lewatit M-62 (86.5 mg/g) [81], Lewatit MP-610 (88.5 mg/g) [81], and Amberlite IRA-900 (150 mg/g) [82].

Table 1

More interestingly, the thermodynamic parameters for Cr(VI) adsorption onto LDH presented in **Table 2** demonstrated that almost every adsorption process occurred spontaneously ($\Delta G° < 0$) and endothermically ($\Delta H° > 0$) within the reported experiment conditions. This means that the equilibrium constant of adsorption increased when the solution temperature also increased. As well, the positive $\Delta S°$ value in most observation cases indicates that the organization of chromium at the solid/solution interface during the adsorption process becomes more random.

Table 2

7. Conclusions

On the basis of the above discussions, we put forward the following vital conclusions and future perspectives:

- Among the existing preparation methods of layered double hydroxides, co-precipitation is the most common one because of its simplicity in creating LDH with a high crystalline structure.

- Layered double hydroxides are a non-porous material with a low specific surface area (1.80–179 m^2/g); therefore, the pore filling's contribution to the chromium adsorption mechanism is insignificant.

- Layered double hydroxides can be classified as a dual-electronic adsorbent. They have positively charged external surfaces (pH_{IEP} >9.0) and high anionic exchange capacity (53–520 meq/100g). A high density of positive charges contributes to adsorbing Cr(VI) anions through the electrostatic attraction. Meanwhile, the host interlayer anions (Cl^-, NO_3^-, SO_4^{2-}, and CO_3^{2-}) plays a key role in the adsorption mechanism of hexavalent chromium anions in solution through the anion exchange.

- Adsorption-coupled reduction also plays an integral role in the adsorption mechanism. LDH adsorbs the reduced Cr(III) cations through the processes as isomorphic substitution or/and complexation.

- The Langmuir maximum adsorption capacity of LDH-based materials is obtained within the range between 16.3 mg/g and 726 mg/g.

- Most the adsorption processes of Cr(VI) by LDH-based adsorbent occur spontaneously ($\Delta G° < 0$) and endothermically ($\Delta H° > 0$) and increase the randomness ($\Delta S° > 0$) in the system.

It can therefore be concluded that LDH-based materials have much potential as an adsorbent with a high affinity to toxic chromium in water and wastewater. Future studies should involve in the application of applying these materials to remove Cr(VI) from water, and attempts should be made to explore the states of chromium oxidation on the chromium-laden material.

References

[1] S. Chatterjee, H.N. Tran, O.-B. Godfred, S.H. Woo, Supersorption capacity of anionic dye by newer chitosan hydrogel capsules via green surfactant exchange method, ACS Sustain. Chem. Eng. 6 (2018) 3604–3614.

[2] P. Rajasulochana, V. Preethy, Comparison on efficiency of various techniques in treatment of waste and sewage water – A comprehensive review, Resource–Efficient Technologies 2 (2016) 175–184.

[3] C. Santhosh, V. Velmurugan, G. Jacob, S.K. Jeong, A.N. Grace, A. Bhatnagar, Role of nanomaterials in water treatment applications: A review, Chem. Eng. J. 306 (2016) 1116–1137.

[4] F. Lu, D. Astruc, Nanomaterials for removal of toxic elements from water, Coord. Chem. Rev . 356 (2018) 147–164.

[5] Y. Li, B. Gao, T. Wu, D. Sun, X. Li, B. Wang, F. Lu, Hexavalent chromium removal from aqueous solution by adsorption on aluminum magnesium mixed hydroxide, Water Res. 43 (2009) 3067–3075.

[6] H.N. Tran, C.-C. Lin, H.-P. Chao, Amino acids-intercalated Mg/Al layered double hydroxides as dual–electronic adsorbent for effective removal of cationic and oxyanionic metal ions, Sep. Purif. Technol. 192 (2018) 36–45.

[7] S.-T. Lin, H.N. Tran, H.-P. Chao, J.-F. Lee, Layered double hydroxides intercalated with sulfur-containing organic solutes for efficient removal of cationic and oxyanionic metal ions, Appl. Clay Sci. 162 (2018) 443–453.

[8] C. Lei, X. Zhu, B. Zhu, C. Jiang, Y. Le, J. Yu, Superb adsorption capacity of hierarchical calcined Ni/Mg/Al layered double hydroxides for Congo red and Cr(VI) ions, J. Hazard. Mater. 321 (2017) 801–811.

[9] Y. Lu, B. Jiang, L. Fang, F. Ling, J. Gao, F. Wu, X. Zhang, High performance NiFe layered double hydroxide for methyl orange dye and Cr(VI) adsorption, Chemosphere 152 (2016) 415–422.

[10] L. Deng, Z. Shi, L. Wang, S. Zhou, Fabrication of a novel $NiFe_2O_4$/Zn-Al layered double hydroxide intercalated with EDTA composite and its adsorption behavior for Cr(VI) from aqueous solution, J. Phys. Chem. Solids 104 (2017) 79–90.

[11] L. Deng, Z. Shi, X. Peng, Adsorption of Cr(vi) onto a magnetic $CoFe_2O_4$/MgAl-LDH composite and mechanism study, RSC Adv. 5 (2015) 49791–49801.

[12] V.R.L. Constantino, T.J. Pinnavaia, Basic Properties of $Mg^{2+}1–xAl^{3+}x$ Layered Double Hydroxides Intercalated by Carbonate, Hydroxide, Chloride, and Sulfate Anions, Inorg. Chem. 34 (1995) 883–892.

[13] N.K. Lazaridis, D.D. Asouhidou, Kinetics of sorptive removal of chromium(VI) from aqueous solutions by calcined Mg-Al-CO_3 hydrotalcite, Water Res. 37 (2003) 2875–2882.

[14] D. Park, S.–R. Lim, Y.-S. Yun, J.M. Park, Reliable evidences that the removal mechanism of hexavalent chromium by natural biomaterials is adsorption–coupled reduction, Chemosphere 70 (2007) 298–305.

[15] N. Fellenz, F.J. Perez-Alonso, P.P. Martin, J.L. García–Fierro, J.F. Bengoa, S.G. Marchetti, S. Rojas, Chromium (VI) removal from water by means of adsorption–reduction at the surface of amino–functionalized MCM-41 sorbents, Microporous and Mesoporous Mater. 239 (2017) 138–146.

[16] R. Jin, Y. Liu, G. Liu, T. Tian, S. Qiao, J. Zhou, Characterization of Product and Potential Mechanism of Cr(VI) Reduction by Anaerobic Activated Sludge in a Sequencing Batch Reactor, Sci. Rep. 7 (2017) 1681.

[17] B. Choudhary, D. Paul, A. Singh, T. Gupta, Removal of hexavalent chromium upon interaction with biochar under acidic conditions: mechanistic insights and application, Environ. Sci. Pollut. Res. 24 (2017) 16786–16797.

[18] Z. Peng, C. Xiong, W. Wang, F. Tan, Y. Xu, X. Wang, X. Qiao, Facile modification of nanoscale zero-valent iron with high stability for Cr(VI) remediation, Sci. Total Environ. 596–597 (2017) 266–273.

[19] H.-P. Chao, Y.-C. Wang, H.N. Tran, Removal of hexavalent chromium from groundwater by Mg/Al–layered double hydroxides using characteristics of *in-situ* synthesis, Environ. pollut. (2018).

[20] S. Chen, Y. Huang, X. Han, Z. Wu, C. Lai, J. Wang, Q. Deng, Z. Zeng, S. Deng, Simultaneous and efficient removal of Cr(VI) and methyl orange on LDHs decorated porous carbons, Chem. Eng. J. 352 (2018) 306–315.

[21] P. Koilraj, K. Sasaki, Eco–friendly alkali-free arginine-assisted hydrothermal synthesis of different layered double hydroxides and their chromate adsorption/reduction efficiency, ChemistrySelect 2 (2017) 10459–10469.

[22] B. Zhang, L. Luan, R. Gao, F. Li, Y. Li, T. Wu, Rapid and effective removal of Cr(VI) from aqueous solution using exfoliated LDH nanosheets, Colloids Surf. A 520 (2017) 399–408.

[23] L. Ma, S.M. Islam, H. Liu, J. Zhao, G. Sun, H. Li, S. Ma, M.G. Kanatzidis, Selective and Efficient Removal of Toxic Oxoanions of As(III), As(V), and Cr(VI) by Layered Double Hydroxide Intercalated with MoS_4^{2-}, Chem. Mater. 29 (2017) 3274–3284.

[24] K. Zhu, Y. Gao, X. Tan, C. Chen, Polyaniline-Modified Mg/Al Layered Double Hydroxide Composites and Their Application in Efficient Removal of Cr(VI), Acs Sustain. Chem. Eng. 4 (2016) 4361–4369.

[25] X. He, X. Qiu, J. Chen, Preparation of Fe(II)-Al layered double hydroxides: Application to the adsorption/reduction of chromium, Colloids Surf. A 516 (2017) 362–374.

[26] L. Alidokht, S. Oustan, A. Khataee, M. Neyshabouri, A. Reyhanitabar, Removal of chromate from aqueous solution by reduction with nanoscale Fe-Al layered double hydroxide, Res. Chem. Intermed. 44 (2018) 2319–2331.

[27] X. Wang, X. Zhu, X. Meng, Preparation of a Mg/Al/Fe layered supramolecular compound and application for removal of Cr(VI) from laboratory wastewater, RSC Adv. 7 (2017) 34984–34993.

[28] G. Sheng, J. Hu, H. Li, J. Li, Y. Huang, Enhanced sequestration of Cr(VI) by nanoscale zero-valent iron supported on layered double hydroxide by batch and XAFS study, Chemosphere 148 (2016) 227–232.

[29] M. Laipan, H. Fu, R. Zhu, L. Sun, J. Zhu, H. He, Converting Spent Cu/Fe Layered Double Hydroxide into Cr(VI) Reductant and Porous Carbon Material, Sci. Rep. 7 (2017) 7277.

[30] L. Cocheci, P. Barvinschi, R. Pode, E.-M. Seftel, E. Popovici, Chromium(VI) Ion Removal from Aqueous Solutions Using a Zn-Al-Type Layered Double Hydroxide, Adsorpt. Sci. Technol. 28 (2010) 267–279.

[31] H.N. Tran, C.-C. Lin, S.H. Woo, H.–P. Chao, Efficient removal of copper and lead by Mg/Al layered double hydroxides intercalated with organic acid anions: Adsorption kinetics, isotherms, and thermodynamics, Appl. Clay Sci. 154 (2018) 17–27.

[32] X. Yue, W. Liu, Z. Chen, Z. Lin, Simultaneous removal of Cu(II) and Cr(VI) by Mg-–AlCl layered double hydroxide and mechanism insight, J. Environ. Sci. 53 (2017) 16–26.

[33] N. Chubar, V. Gerda, O. Megantari, M. Mičušík, M. Omastova, K. Heister, P. Man, J. Fraissard, Applications versus properties of Mg-Al layered double hydroxides provided by their syntheses methods: Alkoxide and alkoxide-free sol-gel syntheses and hydrothermal precipitation, Chem. Eng. J. 234 (2013) 284–299.

[34] L. Châtelet, J.Y. Bottero, J. Yvon, A. Bouchelaghem, Competition between monovalent and divalent anions for calcined and uncalcined hydrotalcite: anion exchange and adsorption sites, Colloids Surf. A 111 (1996) 167–175.

[35] N. Kumar, L. Reddy, V. Parashar, J.C. Ngila, Controlled synthesis of microsheets of ZnAl layered double hydroxides hexagonal nanoplates for efficient removal of Cr(VI) ions and anionic dye from water, J. Environ. Chem. Eng. 5 (2017) 1718–1731.

[36] N. Chubar, New inorganic (an)ion exchangers based on Mg-Al hydrous oxides: (Alkoxide-free) sol-gel synthesis and characterisation, J. Colloid Interface Sci. 357 (2011) 198–209.

[37] A. Halajnia, S. Oustan, N. Najafi, A.R. Khataee, A. Lakzian, The adsorption characteristics of nitrate on Mg-Fe and Mg-Al layered double hydroxides in a simulated soil solution, Appl. Clay Sci. 70 (2012) 28–36.

[38] L.A. Ramírez-Llamas, R. Leyva-Ramos, A. Jacobo-Azuara, J.M. Martínez-Rosales, E.D. Isaacs-Paez, Adsorption of Fluoride from Aqueous Solution on Calcined and Uncalcined Layered Double Hydroxide, Adsorpt. Sci. Technol. 33 (2015) 393–410.

[39] W. Wang, J. Zhou, G. Achari, J. Yu, W. Cai, Cr(VI) removal from aqueous solutions by hydrothermal synthetic layered double hydroxides: Adsorption performance, coexisting anions and regeneration studies, Colloids Surf. A 457 (2014) 33–40.

[40] S. Abelló, F. Medina, D. Tichit, J. Pérez-Ramírez, J.E. Sueiras, P. Salagre, Y. Cesteros, Aldol condensation of campholenic aldehyde and MEK over activated hydrotalcites, Appl. Catal. B 70 (2007) 577–584.

[41] M. Abdellattif, M. Mokhtar, MgAl-Layered Double Hydroxide Solid Base Catalysts for Henry Reaction: A Green Protocol, Catalysts 8 (2018) 133.

[42] M. Mubarak, H. Jeon, M.S. Islam, C. Yoon, J.S. Bae, S.–J. Hwang, W.S. Choi, H.-J. Lee, One-pot synthesis of layered double hydroxide hollow nanospheres with ultrafast removal efficiency for heavy metal ions and organic contaminants, Chemosphere 201 (2018) 676–686.

[43] F. Ling, L. Fang, Y. Lu, J. Gao, F. Wu, M. Zhou, B. Hu, A novel CoFe layered double hydroxides adsorbent: High adsorption amount for methyl orange dye and fast removal of Cr(VI), Microporous and Mesoporous Mater. 234 (2016) 230–238.

[44] C. Peng, J. Dai, J. Yu, J. Yin, Calcined Mg–Fe layered double hydroxide as an absorber for the removal of methyl orange, AIP Adv. 5 (2015) 057138.

[45] K. Takehira, Recent development of layered double hydroxide-derived catalysts −Rehydration, reconstitution, and supporting, aiming at commercial application−, Appl. Clay Sci. 136 (2017) 112–141.

[46] M. Khitous, Z. Salem, D. Halliche, Effect of interlayer anions on chromium removal using Mg-Al layered double hydroxides: Kinetic, equilibrium and thermodynamic studies, Chin. J. Chem. Eng. 24 (2016) 433–445.

[47] D. Pradhan, L.B. Sukla, M. Sawyer, P.K.S.M. Rahman, Recent bioreduction of hexavalent chromium in wastewater treatment: A review, J. Ind. Eng. Chem. 55 (2017) 1–20.

[48] A.K. Sengupta, D. Clifford, Chromate ion exchange mechanism for cooling water, Ind. Eng. Chem. Fundam. 25 (1986) 249–258.

[49] L.-L. Li, X.-Q. Feng, R.–P. Han, S.-Q. Zang, G. Yang, Cr(VI) removal via anion exchange on a silver–triazolate MOF, J. Hazard. Mater. 321 (2017) 622–628.

[50] D. Mohan, C.U. Pittman, Activated carbons and low cost adsorbents for remediation of tri– and hexavalent chromium from water, J. Hazard. Mater. 137 (2006) 762–811.

[51] N.K. Lazaridis, T.A. Pandi, K.A. Matis, Chromium(VI) Removal from Aqueous Solutions by Mg−Al−CO_3 Hydrotalcite: Sorption-Desorption Kinetic and Equilibrium Studies, Ind. Eng. Chem. Res. 43 (2004) 2209–2215.

[52] E. Álvarez-Ayuso, H.W. Nugteren, Purification of chromium(VI) finishing wastewaters using calcined and uncalcined Mg-Al-CO_3-hydrotalcite, Water Res. 39 (2005) 2535–2542.

[53] T. Hongo, H. Wakasa, A. Yamazaki, Synthesis and adsorption properties of nanosized Mg-Al layered double hydroxides with Cl^-, NO_3^- or SO_4^{2-} as interlayer anion, Mater. Sci–Poland 29 (2011) 86–91.

[54] T. Kameda, E. Kondo, T. Yoshioka, Treatment of Cr(VI) in aqueous solution by Ni-Al and Co-Al layered double hydroxides: Equilibrium and kinetic studies, J. Water Process Eng. 8 (2015) e75–e80.

[55] D. Park, Y.-S. Yun, J.M. Park, Studies on hexavalent chromium biosorption by chemically–treated biomass of Ecklonia sp, Chemosphere 60 (2005) 1356–1364.

[56] D. Park, Y.-S. Yun, D.S. Lee, J.M. Park, Optimum condition for the removal of Cr(VI) or total Cr using dried leaves of Pinus densiflora, Desalination 271 (2011) 309–314.

[57] I. Ikemoto, K. Ishii, S. Kinoshita, H. Kuroda, M.A. Alario Franco, J.M. Thomas, X-ray photoelectron spectroscopic studies of CrO_2 and some related chromium compounds, J. Solid State Chem. 17 (1976) 425–430.

[58] H.N. Tran, Comment on "simultaneous and efficient removal of Cr(VI) and methyl orange on LDHs decorated porous carbons", Chem. Eng. J. 359 (2019) 810–812.

[59] H.N. Tran, V.V. Pham, D.-V.N. Vo, P.T. Nguyen, Comment on "Removal of hexavalent chromium by biochar supported nZVI composite: Batch and fixed-bed column evaluations, mechanisms, and secondary contamination prevention", Chemosphere (2019).

[60] J. Zhang, Y. Li, J. Zhou, D. Chen, G. Qian, Chromium (VI) and zinc (II) waste water co-treatment by forming layered double hydroxides: Mechanism discussion via two different processes and application in real plating water, J. Hazard. Mater. 205–206 (2012) 111–117.

[61] S. Deng, Y.P. Ting, Polyethylenimine–Modified Fungal Biomass as a High-Capacity Biosorbent for Cr(VI) Anions: Sorption Capacity and Uptake Mechanisms, Environ. Sci. Technol. 39 (2005) 8490–8496.

[62] A. Olad, R. Nabavi, Application of polyaniline for the reduction of toxic Cr(VI) in water, J. Hazard. Mater. 147 (2007) 845–851.

[63] T. Kameda, E. Kondo, T. Yoshioka, Preparation of Mg-Al layered double hydroxide doped with Fe^{2+} and its application to Cr(VI) removal, Sep. Purif. Technol. 122 (2014) 12–16.

[64] G. Qu, L. Kou, T. Wang, D. Liang, S. Hu, Evaluation of activated carbon fiber supported nanoscale zero–valent iron for chromium (VI) removal from groundwater in a permeable reactive column, J. Environ. Manage. 201 (2017) 378–387.

[65] X. Yuan, Y. Wang, J. Wang, C. Zhou, Q. Tang, X. Rao, Calcined graphene/MgAl-layered double hydroxides for enhanced Cr(VI) removal, Chem. Eng. J. 221 (2013) 204–213.

[66] J. Wang, X. Wang, G. Zhao, G. Song, D. Chen, H. Chen, J. Xie, T. Hayat, A. Alsaedi, X. Wang, Polyvinylpyrrolidone and polyacrylamide intercalated molybdenum disulfide as adsorbents for enhanced removal of chromium(VI) from aqueous solutions, Chem. Eng. J. 334 (2018) 569–578.

[67] M. Aoyama, Comment on "Biosorption of chromium(VI) from aqueous solution by cone biomass of Pinus sylvestris", Bioresour. Technol. 89 (2003) 317–318.

[68] D. Park, Y.-S. Yun, J.M. Park, Comment on "Chromate ion adsorption by agricultural by-products modified with dimethyloldihydroxylethylene urea and choline chloride" by Wartelle and Marshall, Water Res. 40 (2006) 1501–1504.

[69] D. Park, Y.-S. Yun, J.M. Park, Comment on the removal mechanism of hexavalent chromium by biomaterials or biomaterial-based activated carbons, Ind. Eng. Chem. Res. 45 (2006) 2405–2407.

[70] H.N. Tran, S.-J. You, A. Hosseini-Bandegharaei, H.-P. Chao, Mistakes and inconsistencies regarding adsorption of contaminants from aqueous solutions: A critical review, Water Res. 120 (2017) 88–116.

[71] D. Park, Y.-S. Yun, J.M. Park, Mechanisms of the removal of hexavalent chromium by biomaterials or biomaterial-based activated carbons, J. Hazard. Mater. 137 (2006) 1254–1257.

[72] B. Saha, C. Orvig, Biosorbents for hexavalent chromium elimination from industrial and municipal effluents, Coord. Chem. Rev. 254 (2010) 2959–2972.

[73] D. Park, Y.-S. Yun, J.Y. Kim, J.M. Park, How to study Cr(VI) biosorption: Use of fermentation waste for detoxifying Cr(VI) in aqueous solution, Chem. Eng. J. 136 (2008) 173–179.

[74] K.K. Singh, S.H. Hasan, M. Talat, V.K. Singh, S.K. Gangwar, Removal of Cr (VI) from aqueous solutions using wheat bran, Chem. Eng. J. 151 (2009) 113–121.

[75] H.-P. Chao, Y.-C. Wang, H.N. Tran, Removal of hexavalent chromium from groundwater by Mg/Al–layered double hydroxides using characteristics of *in-situ* synthesis, Environ. pollut. 243 (2018) 620–629.

[76] J.L. Gardea-Torresdey, K.J. Tiemann, V. Armendariz, L. Bess-Oberto, R.R. Chianelli, J. Rios, J.G. Parsons, G. Gamez, Characterization of Cr(VI) binding and reduction to Cr(III) by the agricultural byproducts of *Avena monida* (Oat) biomass, J. Hazard. Mater. 80 (2000) 175–188.

[77] Y.-L. Wei, Y.-C. Lee, H.-F. Hsieh, XANES study of Cr sorbed by a kitchen waste compost from water, Chemosphere 61 (2005) 1051–1060.

[78] B. Volesky, Biosorption and me, Water Res. 41 (2007) 4017–4029.

[79] T.N. Hai, Comments on “Effect of temperature on the adsorption of methylene blue dye onto sulfuric acid-treated orange peel”, Chem. Eng. Commun. 204 (2017) 134–139.

[80] I. Langmuir, The adsorption of gases on plane surfaces of glass, mica and platinum, J. Am. Chem. Soc. 40 (1918) 1361–1403.

[81] F. Gode, E. Pehlivan, Removal of Cr(VI) from aqueous solution by two Lewatit-anion exchange resins, J. Hazard. Mater. 119 (2005) 175–182.

[82] S.-C. Lee, J.-K. Kang, E.-H. Sim, N.-C. Choi, S.–B. Kim, Modacrylic anion-exchange fibers for Cr(VI) removal from chromium-plating rinse water in batch and flow-through column experiments, J. Environ. Sci. Health., Part A 52 (2017) 1195–1203.

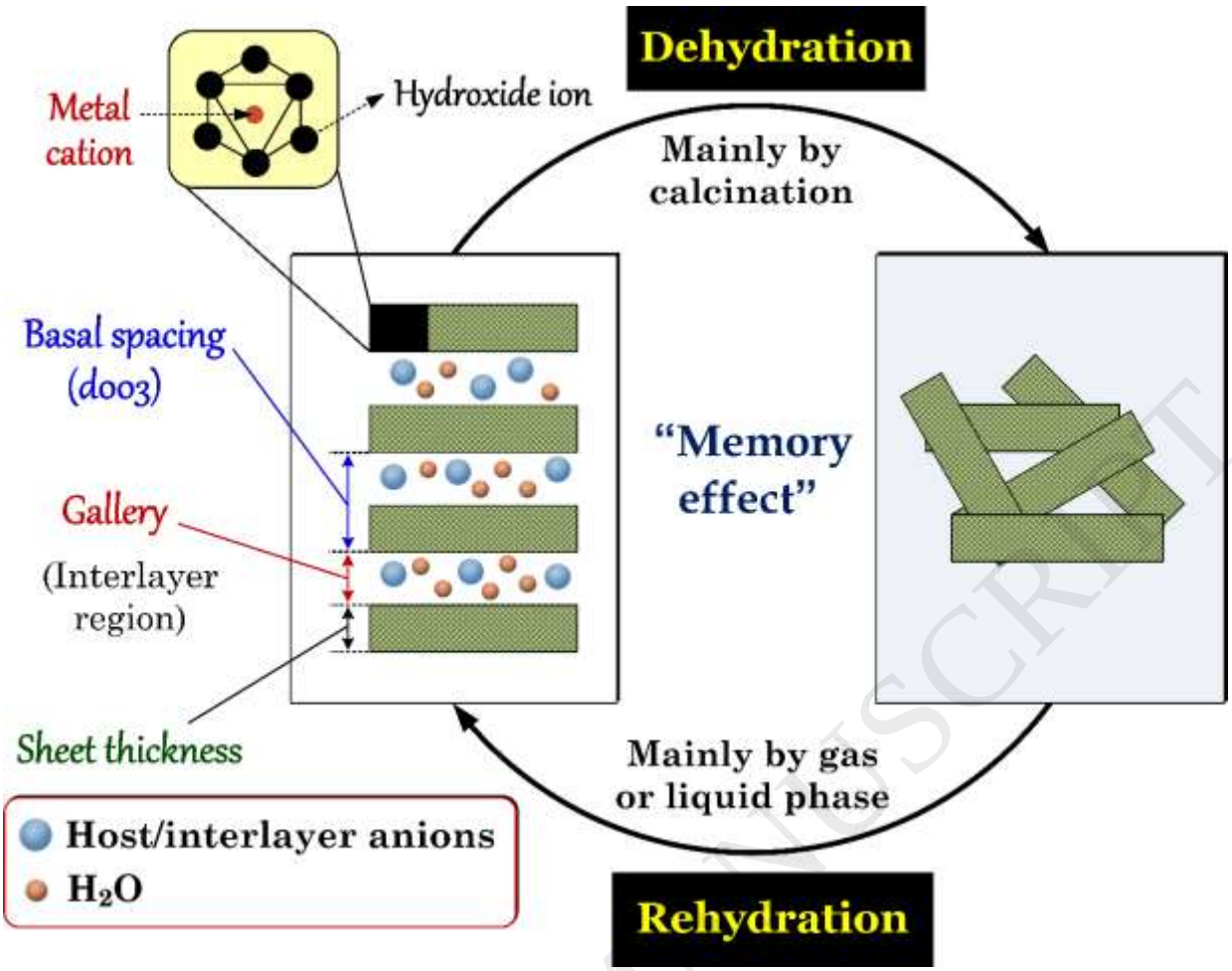

Figure 1. A typical crystal structure of LDH, dehydration of LDH by calcination, and rehydration of calcined LDH

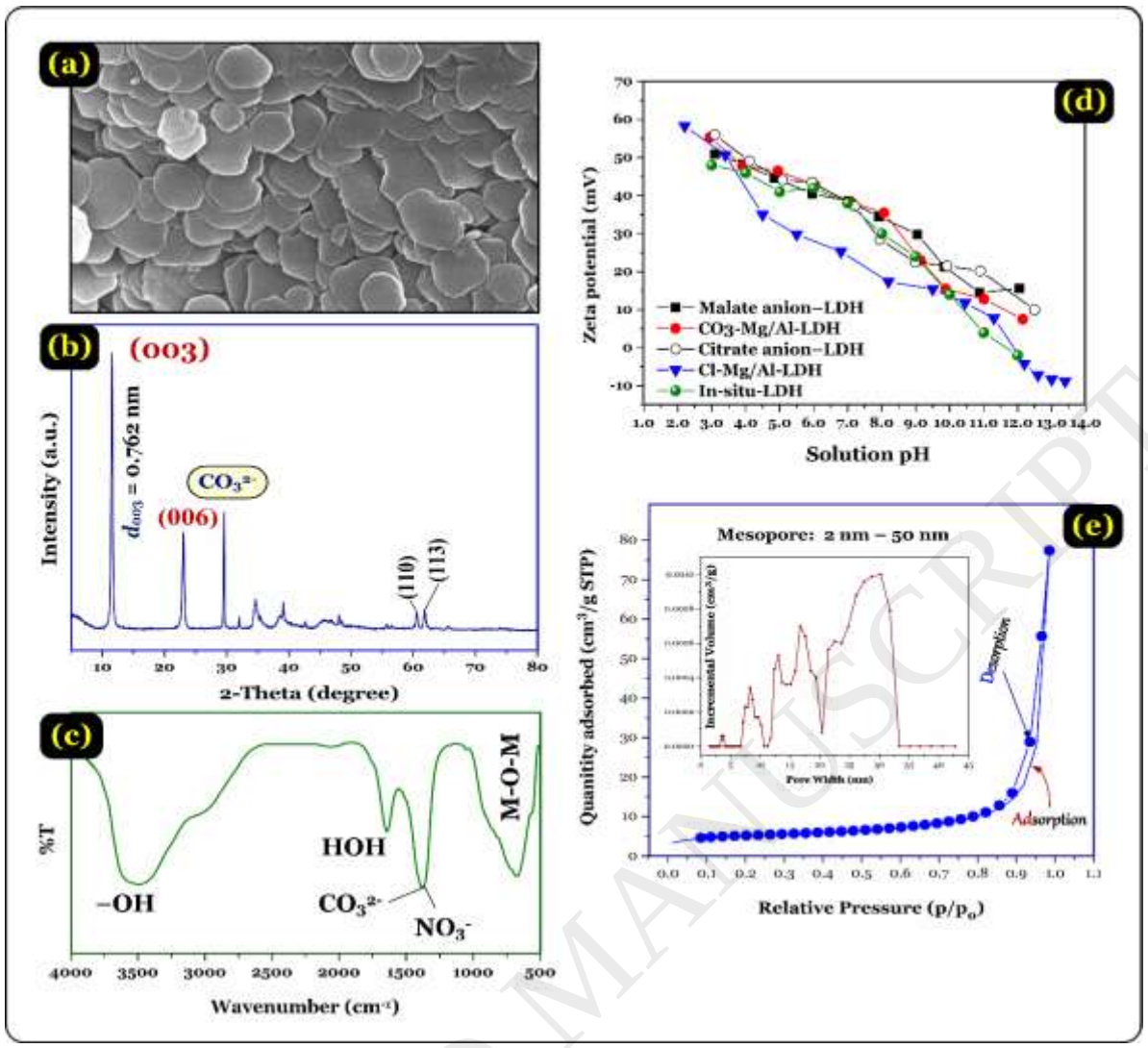

Figure 2. Some typical properties of layered double hydroxides characterized by: **(a)** SEM image of CO_3-Mg/Al-LDH [31], **(b)** XRD pattern of CO_3-Mg/Al-LDH [19], **(c)** FTIR of CO_3-Mg/Al-LDH [31], **(d)** zeta potential of Cl-Mg/Al-LDH [28], CO_3-Mg/Al-LDH, citrate anion-intercalated Mg/Al-LDH, malate anion-intercalated Mg/Al-LDH [31], and in-situ-LDH [19], and **(e)** nitrogen adsorption/desorption isotherm of CO_3-Mg/Al-LDH (an insert figure representing its pore size distribution) [7]

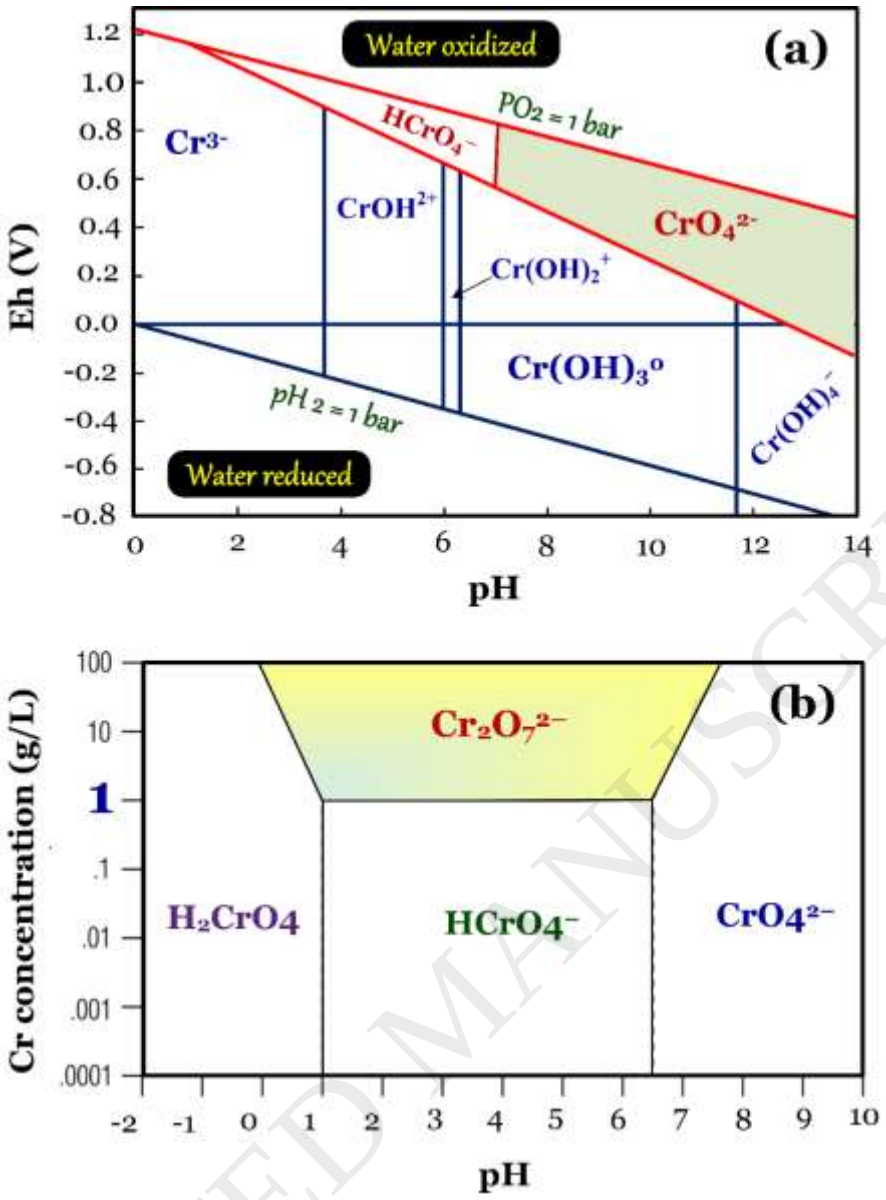

Figure 3. (a) h–pH diagram for chromium [50], and **(b)** relative distribution of Cr(VI) species in water as a function of pH and Cr(VI) concentration [48]

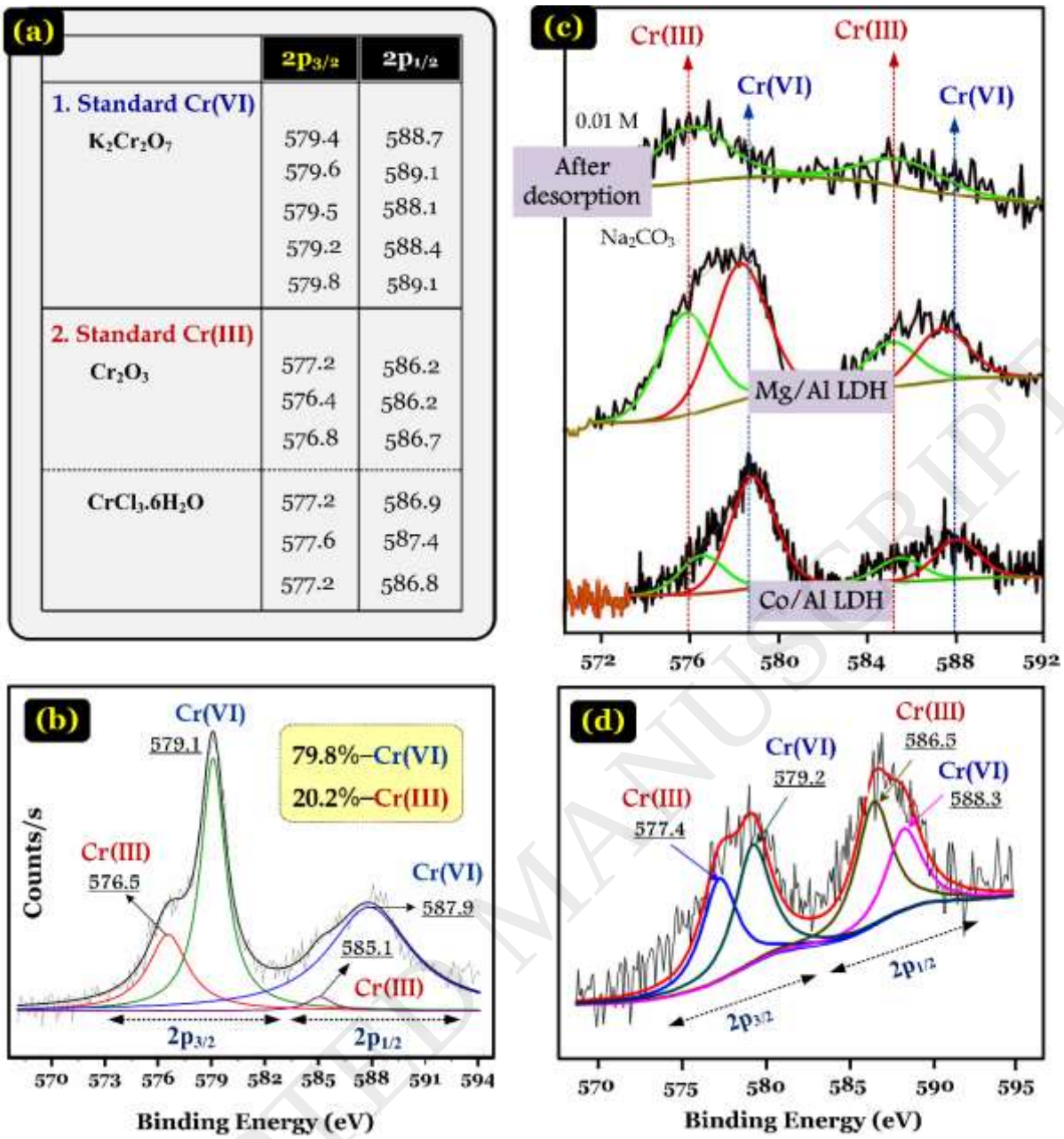

Figure 4. (a) Corresponding binding energies of the Cr(VI) and Cr(III) standards [16, 17, 23, 56, 57]; a typical Cr 2p spectrum after Cr(VI) adsorption of **(b)** *in-situ*-Mg/AL-LDH [19], **(c)** amino acid-intercalated Co/Al-LDH and amino acid-intercalated Mg/Al-LDH [21]; and **(d)** $NiFe_2O_4$-Zn/Al-LDH [10].

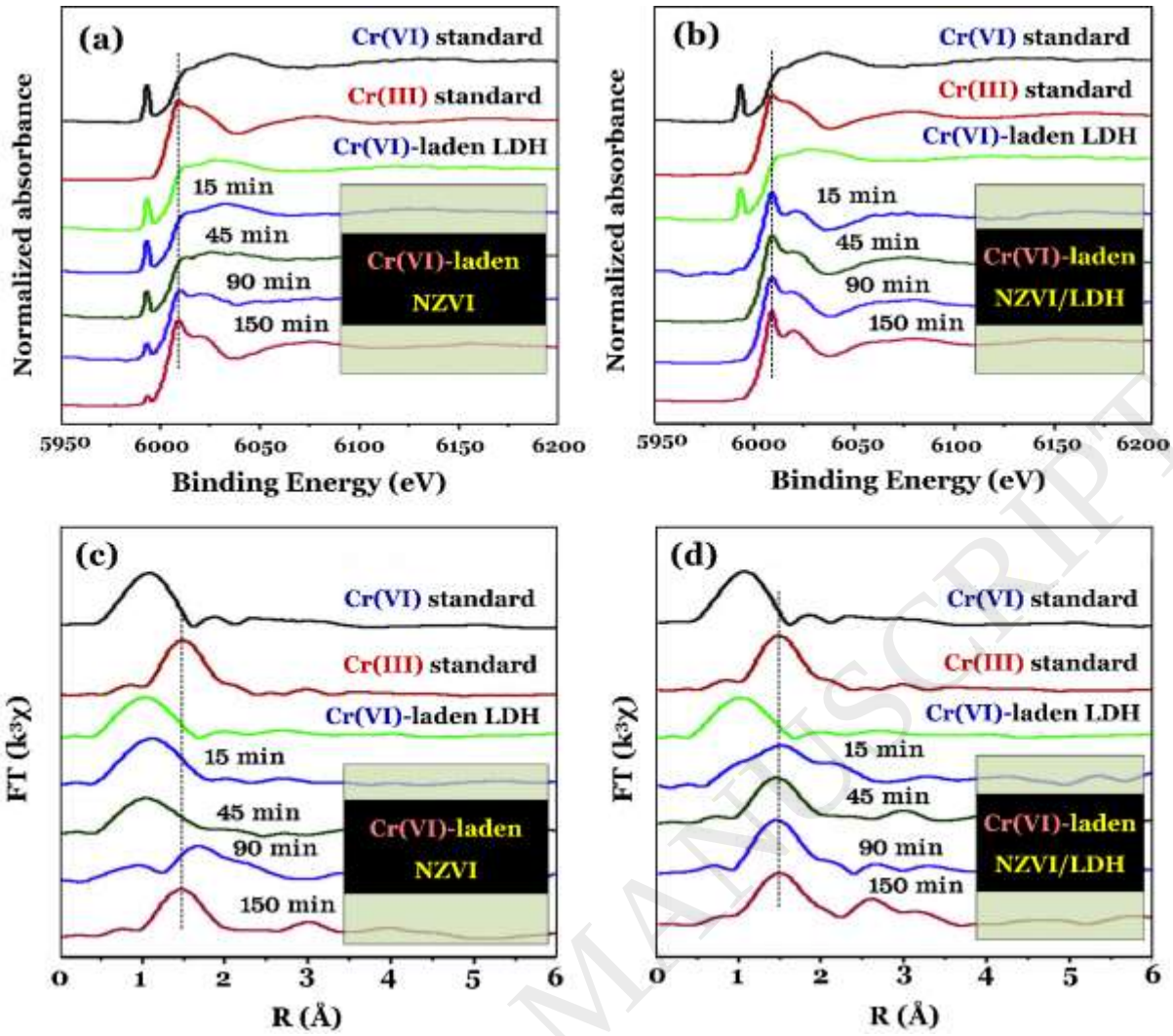

Figure 5. (a–b) Cr K-edge XANES spectra of the Cr(VI) and Cr(III) standards, Cr(VI)-adsorbed Mg/Al-LDH, Cr(VI)-adsorbed nanoscale zero-valent iron (NZVI), and Cr(VI)-adsorbed NZVI/LDH; and **(c–d)** K-edge EXAFS spectra of the Cr(VI) and Cr(III) standards, Cr(VI)-adsorbed Mg/Al-LDH, Cr(VI)-adsorbed nanoscale zero-valent iron (NZVI), and Cr(VI)-adsorbed NZVI/LDH [28]

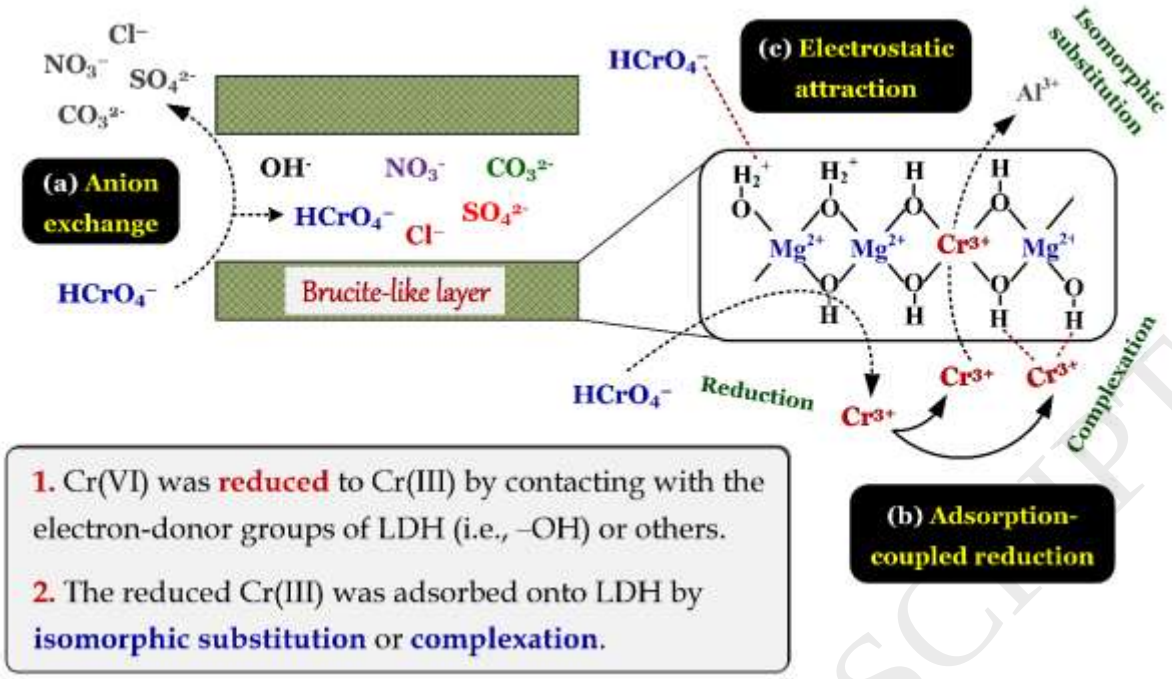

Figure 6. Possible adsorption mechanism of Cr(VI) onto a typical Mg/Al-LDH (excluding the case of intercalation with organic or inorganic anions, modification with polymer, or presence of iron component)

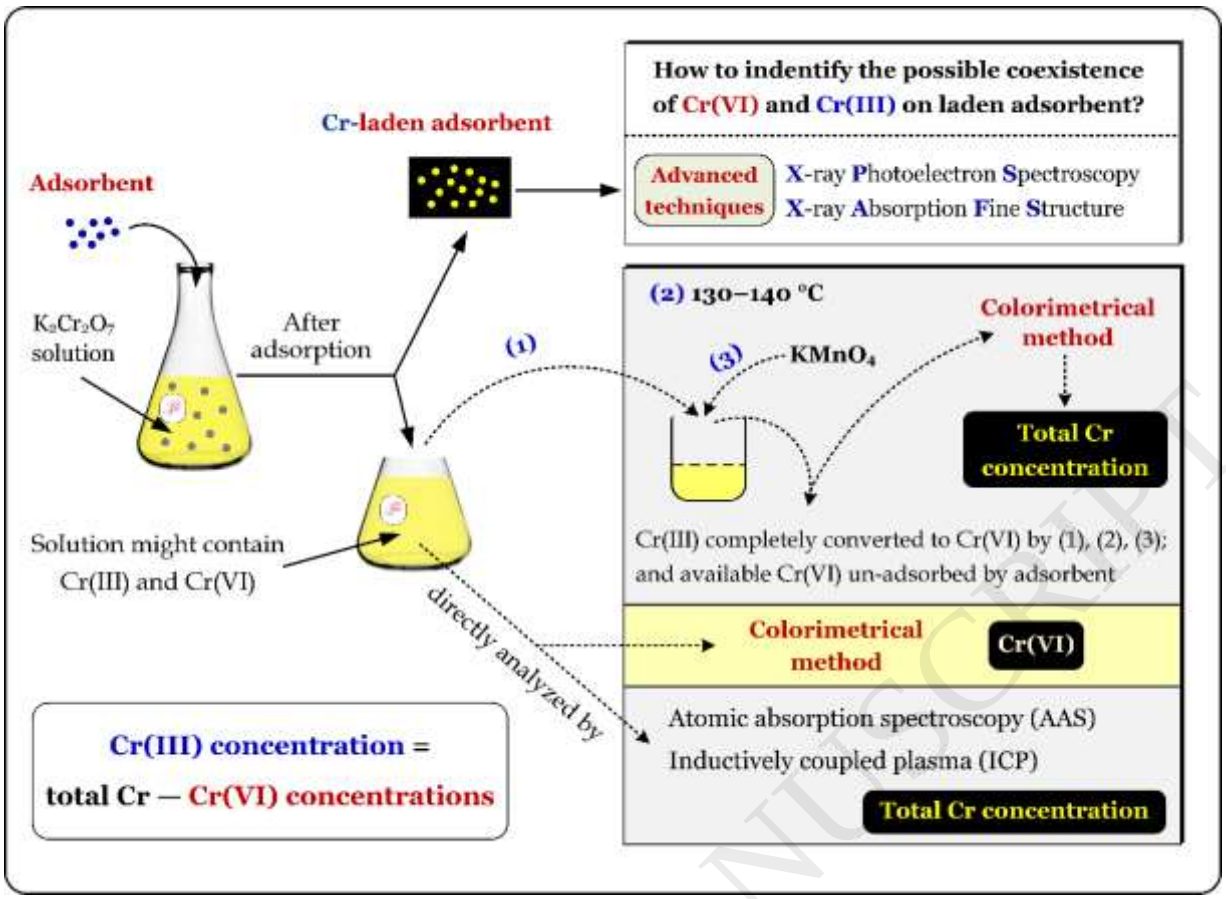

Figure 7. Determination of the presence of different species of chromium in solid and liquid phases

Table 1. The Langmuir maximum adsorption capacity (Q^{o}_{max}) of Cr(VI) from water environment

LDH	Interlayer anion	Treatment	Adsorption condition					Q^{o}_{max} (mg/g)	Ref.
			m/V (g/L)	pH	T (°C)	t (h)	Co (mg/L)		
Laboratory synthetic water									
Mg/Al/Fe	NO_3^-, SO_4^{2-}	400 °C	4.0	9.0	NA	—	50–6000	726	[27]
Mg/Al	Cl^-	Fe^{2+}	10	NA	30	24	5–1000	649	[63]
Mg/Al	NO_3^-	Polyaniline	0.2	3.0	30	24	5–120	435	[24]
Mg/Al	CO_3^{2-}	—	2.0	12	25	24	100–900	339	[19]
Mg/Al	CO_3^{2-}	—	2.0	5.0	25	24	100–900	246	[19]
Ni/Al	NO_3^-	[b]AC	0.2	2.0	30	—	20–250	236	[20]
Mg/Al	NO_3^-	400 °C	4.0	9.0	NA	—	50–6000	199	[27]
Mg/Al	NO_3^-	Graphene	1.0	NA	NA	24	50–250	184	[65]
Zn/Al	Cl^-	—	0.8	5.0	25	12	50–350	172	[35]
Mg/Fe	—	400 °C	1.0	NA	25	0.3	10–300	137	[42]
Mg/Al	MoS_4^{2-}	—	1.0	NA	RT	24	10–400	130	[23]
Mg/Fe	—	—	1.0	NA	25	0.3	10–300	129	[42]
Mg/Al	Cl^-	—	2.0	4.0	30	2.5	5–200	110	[5]
Ni–Al	Cl^-	—	10	NA	30	24	260–1300	104	[54]
Ni/Mg/Al	SO_4^-	[a]600 °C	0.5	NA	30	24	20–100	103	[8]
Co–Al	Cl^-	—	10	NA	30	24	260–1300	98.8	[54]
Mg/Al	Arginine	—	1.0	8.0	25	3.0	25–510	84.2	[21]
Co/Al	Arginine	—	1.0	8.0	25	3.0	25–510	77.8	[21]
Mg/Al	NO_3^-	—	2.0	6.0	20	2.0	5–200	71.9	[46]
Zn/Al	NO_3^-	—	0.2	6.5	25	24	30–55	68.1	[39]
Zn/Al	[c]EDTA	$NiFe_2O_4$	2.0	6.0	25	2.0	10–1000	66.1	[10]
Mg/Al	NO_3^-	$CoFe_2O_4$	3.0	2.0	30	24	55–250	65.7	[11]
Mg/Al	Cl^-	—	2.0	6.0	20	2.0	5–200	58.8	[46]
Mg/Al	NO_3^-	—	0.2	3.0	15	24	5–120	58.8	[24]
Ni/Al	NO_3^-	—	0.2	6.5	25	24	30–55	57.5	[39]
Zn/Al	Arginine	—	1.0	8.0	25	3.0	25–510	55.9	[21]
Mg/Al	SO_4^{2-}	—	2.0	6.0	20	2.0	5–200	55.6	[46]
Ni/Mg/Al	SO_4^-	—	0.5	NA	30	24	20–100	49.6	[8]
Ni/Al	NO_3^-	—	0.2	2.0	30	NA	20–250	34.1	[20]
Mg/Al	NO_3^-	—	0.2	6.5	25	24	30–55	30.3	[39]
Co/Fe	CO_3^{2-}	—	0.2	7.5	25	2.0	2–25	27.6	[43]
Ni/Fe	NO_3^-	—	0.2	NA	RT	4.0	4–20	26.8	[9]
Mg/Al	CO_3^{2-}	—	1.0	6.0	30	4.0	5–100	17.0	[51]
Real wastewater									
Finishing wastewater									
Mg/Al	CO_3^{2-}	[a]600 °C	2.0	1.2	RT	24	57–448	128	[52]
Mg/Al	CO_3^{2-}	—	2.0	1.2	RT	1.0	11–57	16.3	[52]
Plating wastewater									
Ca/Al	Cl^-	—	4.0	NA	RT	NA	10–420	62.3	[60]

Note: [a]Calcinated temperature, [b]AC (activated carbon derived from oil-tea shells), [c]EDTA (ethylenediaminetetraacetic acid), RT (room temperature), and NA (not reported).

Table 2. Thermodynamic parameters for Cr(VI) adsorption process onto various kinds of LDH

	Treatment	T (K)	ΔG° (kJ/mol)	ΔH° (kJ/mol)	ΔS° (kJ/mol×K)	Ref.
Ni/Mg/Al	—	293	−6.26	17.7	0.085	[5]
		303	−8.21			
		313	−8.96			
Ni/Mg/Al	—	293	8.35	22.1	0.047	[8]
		303	7.88			
		313	7.41			
Ni/Mg/Al	600 °C	293	4.07	21.7	0.060	[8]
		303	3.47			
		313	2.87			
Ni/Al	PAB	293	−3.98	60.6	0.115	[20]
		303	−4.63			
		313	−5.18			
Zn/Al	—	298	−11.7	46.5	0.171	[35]
		308	−14.2			
		318	−17.0			
$NiFe_2O_4$/Zn-Al	—	298	−4.72	2.91	0.026	[10]
		308	−5.06			
		318	−5.23			
Mg/Al	Polyaniline	288	−11.8	18.4	0.095	[24]
		303	−13.2			
		318	−15.1			
Mg/Al	—	293	−24.4	4.990	0.100	[46]
		303	−25.5			
		313	−26.4			
Mg/Al	—	288	−6.49	46.3	0.183	[22]
		298	−8.04			
		308	−10.2			
Mg/Al	Graphene	293	−4.17	16.9	0.072	[65]
		303	−4.51			
		313	−5.64			
Mg/Al	$CoFe_2O_4$	283	−1.14	−7.18	−0.021	[11]
		303	−0.71			
		233	−0.28			

Note: The Gibbs energy change ($\Delta G°$) can be directly calculated from the equation of $\Delta G° = –RT \times \ln K_C$. Meanwhile, the enthalpy change ($\Delta H°$) and the entropy change ($\Delta S°$) are calculated from the slope and intercept of the well-known van't Hoff equation of $\ln K_C = (–\Delta H°/R)1/T + \Delta S°/R$; where K_C is the equilibrium constant, R is the gas constant (8.314 J/mol × K), and T is temperature in Kelvin.